J. Fluid Mech. (2000), *vol.* 419, *pp.* 203–238. Printed in the United Kingdom

Purely erosional cyclic and solitary steps created by flow over a cohesive bed

By GARY PARKER[1] AND NORIHIRO IZUMI[2]†

[1]St Anthony Falls Laboratory, University of Minnesota, Minneapolis, MN 55414, USA

[2]Department of Civil Engineering, Tohoku University, Sendai 980–8579, Japan

(Received 8 December 1998 and in revised form 16 May 2000)

An erodible surface exposed to supercritical flow often devolves into a series of steps that migrate slowly upstream. Each step delineates a headcut with an associated hydraulic jump. These steps can form in a bed of cohesive material which, once eroded, is carried downstream as washload without redeposition. Here the case of purely erosional, one-dimensional periodic, or cyclic steps in cohesive material is considered. The St. Venant shallow-water equations combined with a formulation for sediment erosion are used to construct a complete theory of the erosional case. The solution allows wavelength, wave height, migration speed and bed and water surface profiles to be determined as functions of imposed parameters. The analysis also admits a solution for a solitary step, or single headcut of self-preserving form.

1. Introduction

It has long been known that the initial period of channel incision on a hillslope swale is often characterized by a series of step-like upstream-migrating headcuts, or gully heads within the channel (e.g. Leopold & Miller 1956). An example of such discontinuous headcuts is provided by the Greyfox channel studied by Reid (1989), shown in figure 1, where 19 gully heads can be discerned. These features have been observed by many other authors, e.g. Blong (1970) and Montgomery & Dietrich (1989); a comprehensive literature review is provided by Reid (1989). Figure 1 suggests that discontinuous headcuts are not due to random irregularities, but are rather an inherent feature of the interaction of water and sediment on steep slopes. It furthermore suggests that there may be an inherent periodicity, or cyclicity associated with this interaction which leads to a characteristic wavelength and wave height for the train of step-like headcuts. These possibilities are pursued in this paper. The phenomenon itself is referred to herein as cyclic steps.

Even the simplest manifestation of the phenomenon in the field, however, involves complications that may contribute without being essential. For example, the headcuts of figure 1 are incised into a grassland hillslope. Those places where the soil surface is covered with grass are likely to offer more resistance to erosion than those that are bare. This variation in erodibility may in turn promote the formation of undercut plunge pools. In addition, while the channels are incisional in the overall sense, some deposition is often observed downstream of each headcut. The headcuts may respond differently to flows of different magnitude. Finally, the crescentic planform shape of

† Present address: School of Civil Engineering, Asian Institute of Technology, Pathumthani 12120, Thailand.

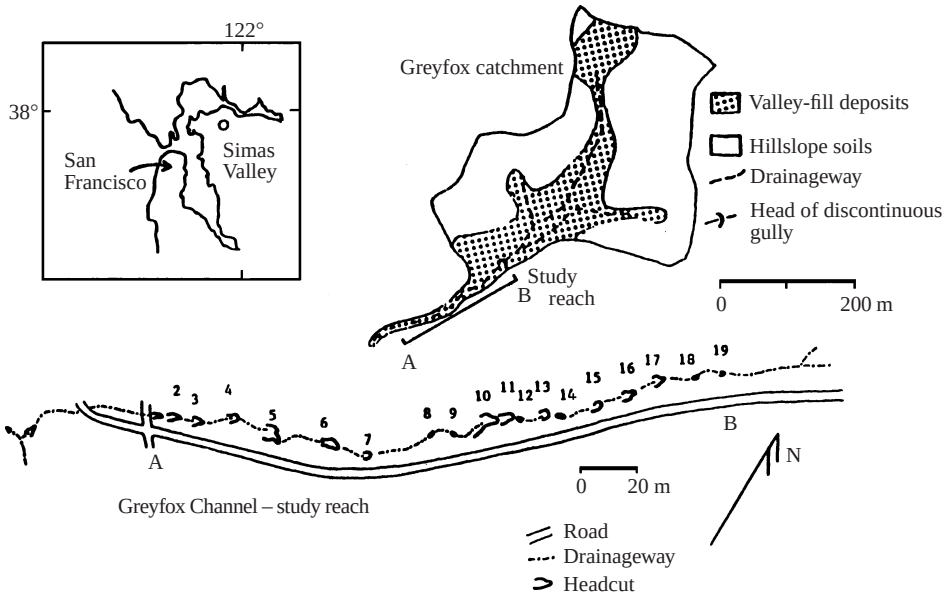

FIGURE 1. Illustration of the Greyfox channel, an incisional channel in a hillslope swale near Simas Valley, California, USA showing 19 discontinuous headcuts. From Reid (1989).

each headcut scarp in figure 1 suggests an element of two-dimensionality in the flow that sculpted it. Here the problem is simplified to its bare essentials by considering a constant one-dimensional flow over a bed of cohesive material of completely uniform erodibility. It is assumed that once material is eroded, it immediately breaks down into a fine-grained washload that is carried out of the reach in question without redeposition. If it can be shown that cyclic steps form under even these restrictive conditions, then their origin can be ascribed to an inherent interaction of water with an erodible bed, rather than to random variation in e.g. erodibility.

Purely erosional cyclic steps have been produced in the laboratory by Sawai (1977) (see also Ashida & Sawai 1977) and Koyama & Ikeda (1998). Sawai introduced flows in channels that were initially rectangular and straight with a width of 1 cm. The channels were cut into a bed consisting of a mixture of bentonite and sand so as to have steep slopes that were constant in the streamwise direction. The quasi-uniform flow preceding the evolution of steps was invariably supercritical in the Froude sense. Within time, the channel bed devolved into a series of steps, each characterized by a short, extremely steep waterfall-like zone of supercritical flow ending in a hydraulic jump. In addition, the channels developed an element of planform sinuosity due to the fact that the sidewalls were erodible. Experimental conditions and results are summarized in table 1. The longitudinal bed profiles of some of the runs are shown in figure 2. The data of table 1 will be used later to test the theory developed here.

More recently Koyama & Ikeda (1998) produced erosional cyclic steps incised into mildly cohesive crushed rock. The crushed rock was composed predominantly of silt, but with some material as large as pea gravel. An example of the cyclic steps produced in their experiments is given in figure 3.

Koyama & Ikeda (1998) point out an analogy between erosional steps in cohesive material and sequences of steps incised into steep bedrock channels. An example of these bedrock steps is given in figure 4. Although the mechanism for bedrock incision

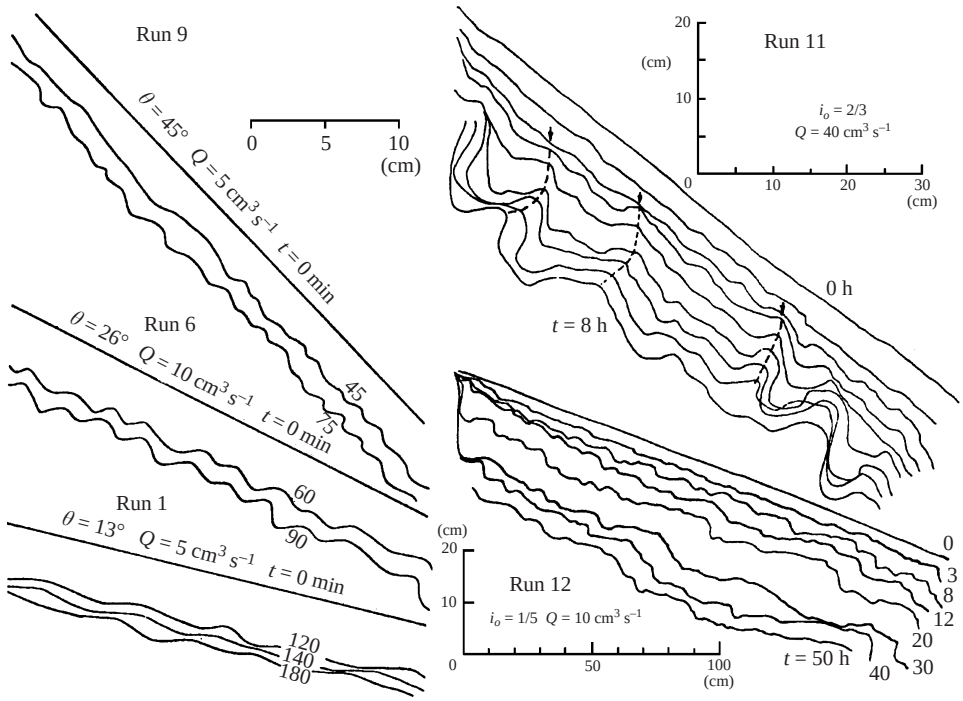

FIGURE 2. Experimental realization of erosional cyclic steps. From Sawai (1977). The initial slope is denoted i_0, the water discharge Q, the initial slope angle θ and time t.

is often rather different from the mechanism for the erosion of cohesive material, it is highly likely that the fundamental flow instability that leads to step formation is the same in both cases.

Cyclic steps form in other contexts as well. Winterwerp *et al.* (1992) have observed essentially the same topography in the case of flow over a relatively steep bed of fine non-cohesive sediment. The observed morphology appears to be related to the chute-and-pool topography described by Simons, Richardsonk & Nordin (1965). In this case there need be no net erosion of the bed. The experiments of Winterwerp *et al.* (1992) indicate that they can form even when the step-averaged rate of sediment transport is constant in the downstream direction, so that the average rate of bed erosion is zero. These steps are here termed transportational cyclic steps, in order to distinguish them from the purely erosional cyclic steps considered below.

Here the case of a fully developed train of finite-amplitude erosional cyclic steps of permanent form is considered. That is, the waveform is assumed to incise and migrate upstream at constant slow rates, while otherwise maintaining a constant topographic expression. The origin of such steps is sought in terms of the purely erosional analogy of the instability known to be responsible for antidunes in the non-cohesive, transportational case.

It is demonstrated in the analysis below that steady, uniform (normal) Froude-super-critical flow over an erodible cohesive bed is inherently unstable under a broad range of conditions. The flow and bed morphology instead devolve into a series of steps that slowly migrate upstream, each delineated by a hydraulic jump. The form of the problem allows for spatially periodic (cyclic) steps that incise and migrate upstream at constant speeds. The analysis is carried to a fully nonlinear level. It is,

Run	Inclination, $\sin\theta$	Discharge ($cm^3\ s^{-1}$)	Water supplying time (h)	Water surface width (cm)	Maximum depth (cm)	Longitudinal		Meander	
						Wave-length (cm)	Wave height (cm)	Wave-length (cm)	Width (cm)
1	0.225	5	3.0	1.3	0.32	8.9	0.93	17.2	0.8
2	0.225	9	3.0	1.2	0.32	6.3	0.97	17.4	1.0
3	0.225	20	2.0	2.2	0.63	5.5	1.15	62.9	0.7
4	0.438	2	3.5	0.9	0.27	3.6	0.34	13.5	1.2
5	0.438	5	2.0	1.3	0.34	4.4	0.79	7.8	2.0
6	0.438	10	1.5	1.7	0.36	4.7	0.96	11.9	1.0
7	0.707	1	0.3			not measured			
8	0.707	2	1.75	0.8	0.21	4.2	0.58	12.7	0.7
9	0.707	5	1.25	1.2	0.35	2.6	0.58	11.9	1.1
10	0.545	10	0.33	1.3	0.39	6.3	2.14	11.8	2.1
11	0.555	40	8.0	3.0	1.2	15	6	15	2.5
12	0.196	10	50.0	1.5	0.56	14	1	11	4.0

TABLE 1. Experimental conditions and results of Sawai's experiments. Note that the wave height in this table does not correspond to the parameter $\Delta\eta_d$ in the analysis, but is instead measured normal to the average slope of the bed. In the case of Run 7, measurement was not conducted because channel deposition was observed.

FIGURE 3. View of experimental cyclic steps produced by Koyama & Ikeda (1998). The width of the channel is approximately 5 cm; the average slope angle is 6°.

FIGURE 4. Bedrock steps in a tributary of the Jin River, China.
The photo is courtesy of E. Kirby.

however, inadequate to describe the formation of plunge pools just downstream of the hydraulic jump.

2. Governing equations

One-dimensional erosional steps are analysed in terms of the St. Venant shallow water equations for momentum and mass balance and the Exner equation for the conservation of bed sediment. The incision rate and migration speed of the steps are assumed to be sufficiently slow to allow for the use of the standard quasi-steady approximation for erodible-bed flow. The balance equations are thus expressed in the following form:

$$u_d \frac{\partial u_d}{\partial x_d} = -g \frac{\partial h_d}{\partial x_d} - g \frac{\partial \eta_d}{\partial x_d} - \frac{\tau_b}{\rho h_d}, \tag{2.1}$$

$$u_d h_d = q_w, \tag{2.2}$$

$$\left(1 - \lambda_p\right) \frac{\partial \eta_d}{\partial t_d} = -E. \tag{2.3}$$

Here h_d, u_d, η_d, t_d and x_d denote flow depth, depth-averaged velocity, bed elevation, time and horizontal downstream distance respectively; the subscript d indicates a dimensional parameter that will later be represented in dimensionless form with the subscript removed. The parameters q_w, λ_p, τ_b, ρ and g denote water discharge

per unit width, bed porosity, boundary shear stress, fluid density and gravitational acceleration. In addition E denotes the volume rate per unit bed area per unit time of the entrainment of sediment into suspension via bed erosion.

The implications and limitations of the above equations must be understood before proceeding. In (2.3) it is implicitly assumed that (*a*) the bed material itself is of uniform erodibility and (*b*) once eroded, the sediment is carried as washload and not redeposited farther downstream. The implication is that the flow never reaches its capacity for carrying sediment within the solution domain. This assumption places limits on the length of the solution domain, because the concentration of suspended sediment cannot rise indefinitely.

The above equations further implicitly assume that (*c*) the suspension is sufficiently dilute to allow the neglect of any effects it might have on the flow dynamics, (*d*) local bed curvature is not so high that a non-hydrostatic contribution to the pressure term becomes important and (*e*) local bed slopes are not too high.

Assumptions (*c*) and (*d*) are not overly restrictive. It will be seen, however, that the bed slope of a profile with cyclic steps can in some cases become quite high just upstream of the hydraulic jump. The formulation of (2.1)–(2.3) can be said to retain dynamic nonlinearities, but to neglect the geometric nonlinearities associated with high bed slope. This simplification, herein termed the infinitesimal-slope formulation, allows a compact theory that is valid over a wide range of conditions. It will be shown later, however, that the inclusion of geometric nonlinearities allows the delineation of an upper bound in friction coefficient on cyclic step formation.

Implicit in the St. Venant equations is the assumption that the phenomenon is 'slender' in some sense. In particular, where L_d denotes the (dimensional) step wavelength and $\tilde{h}$ is a characteristic flow depth, it is necessary that $\tilde{h}/L_d \ll 1$. For most cases of interest cyclic steps will be found to satisfy this condition. As outlined below, however, cyclic steps are closely tied to antidunes, and in fact represent a nonlinear finite-amplitude limiting case. This notwithstanding, antidunes do not always devolve into cyclic steps. This is probably at least partially due to the fact that antidunes are known to form under conditions for which the shallow-water equations do not hold. This issue is elaborated below.

The slender-flow assumption allows the following relation between boundary shear stress τ_b and flow velocity:

$$\tau_b = \rho C_f u_d^2, \tag{2.4}$$

where C_f denotes a dimensionless friction coefficient here approximated as constant for simplicity. The following general form is employed to describe the rate of entrainment of bed sediment into suspension:

$$E = E(\tau_b - \tau_{th}), \tag{2.5}$$

where τ_{th} denotes a threshold boundary shear stress for the onset of bed erosion.

3. Theoretical development

3.1. *Relation for erosion*

Many empirical laws for the erosion of cohesive sediment are found to have the following form:

$$E = \begin{cases} \alpha_1(\tau_b - \tau_{th})^\gamma, & \tau_b > \tau_{th} \\ 0, & \tau_b \leqslant \tau_{th}, \end{cases} \tag{3.1}$$

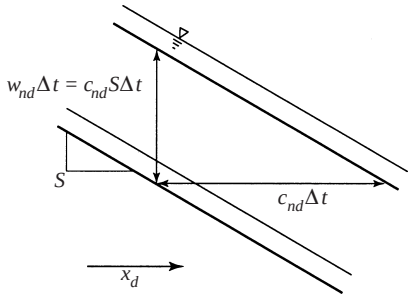

FIGURE 5. Definition diagram for bed erosion in the absence of steps.

where the coefficient α_1 and exponent γ are obtained from tests (e.g. Foster & Meyer 1975). Both are assumed to be positive on physical grounds. Perhaps the most common value of γ found in the literature is 1.0 (e.g. Sheng & Lick 1978; Ariathurai & Arunalandan 1978; Teisson *et al.* 1993; and Howard 1994). Higher values have also commonly been found. For example, Otsubo & Muraoka (1982) report a value of 2.0 for a wide variety of conditions, Umita *et al.* (1988) report values between 1.9 and 2.3 for the early stages of erosion, and Johaneson, Larsen & Petersen (1994) report a value of 4.0. The precise value of the exponent appears to be a function of the 'toughness', or resistance to erosion of the material (Croad 1981). Here the range $\gamma \geqslant 1$ is selected for investigation. Defining a threshold flow velocity u_t such that

$$\tau_{th} = \rho C_f u_t^2, \tag{3.2}$$

(3.1) can be reduced to the following form for $u_d \geqslant u_t$:

$$E = \alpha_1 \tau_{th}^{\gamma} \left(\frac{\tau_b}{\tau_{th}} - 1 \right)^{\gamma} \equiv \alpha \left(\frac{u_d^2}{u_t^2} - 1 \right)^{\gamma}, \tag{3.3}$$

where α now has the dimensions of velocity.

3.2. *Equilibrium flow in the absence of steps*

Before proceeding to an analysis of steps, it is necessary to consider the solution in their absence. To this end a steady, uniform (normal) flow with discharge per unit width q_w over a slowly eroding bed with constant slope S is illustrated in figure 5. Under these conditions (2.1) and (2.2) reduce to

$$C_f Fr_n^2 = S, \quad Fr_n^2 = \frac{u_{nd}^3}{g q_w}. \tag{3.4a, b}$$

Here Fr_n and u_{nd} denote the Froude number and flow velocity associated with this normal flow. Note that for given friction coefficient C_f, if q_w and Fr_n are specified then S and u_{nd} can be computed. If $u_{nd} > u_t$, then the bed is degrading in response to erosion. Denoting the rate of vertical bed degradation in the absence of steps as w_{nd}, (2.3) can be reduced with (3.3) to yield

$$w_{nd} = \frac{\alpha}{1 - \lambda_p} \left(\frac{u_{nd}^2}{u_t^2} - 1 \right)^{\gamma}. \tag{3.5a}$$

It will later prove useful to have a dimensionless version of (3.5*a*). To this end a dimensionless rate of bed degradation in the absence of steps w_n is given as follows:

$$w_n \equiv \frac{(1 - \lambda_p) w_{nd}}{\alpha} = \left(\frac{u_{nd}^2}{u_t^2} - 1 \right)^{\gamma}. \tag{3.5b}$$

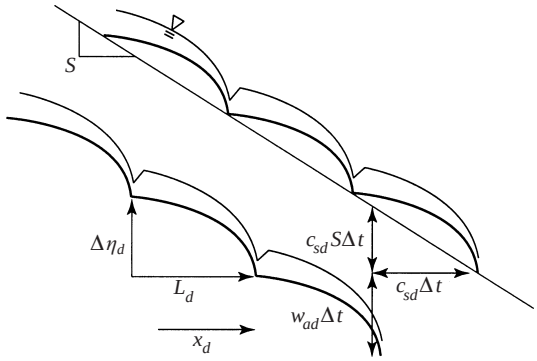

FIGURE 6. Definition diagram for bed erosion in the presence of steps.

As shown in figure 5, a constant rate of upstream migration of the bed profile in the absence of steps c_{nd} can be defined such that

$$w_{nd} = c_{nd}S. \tag{3.6}$$

Any given normal flow with discharge per unit width q_w over an eroding bed with slope S can be compared to another normal flow with the same value of q_w over a lower slope S_t corresponding to the threshold for erosion. From (2.1) and (2.2), S_t can be found from the following relations:

$$S_t = C_f Fr_t^2, \quad Fr_t^2 = \frac{u_t^3}{g q_w}, \tag{3.7a,b}$$

where Fr_t denotes the Froude number at the threshold of motion. Between (3.4a,b) and (3.7a,b) it is seen that

$$\frac{u_{nd}}{u_t} = \left(\frac{Fr_n}{Fr_t}\right)^{2/3} = S_r^{1/3}, \quad S_r = \frac{S}{S_t}. \tag{3.8a,b}$$

These allow the recasting of the relation (3.5b) for bed erosion in the following form;

$$w_n = \left(S_r^{2/3} - 1\right)^{\gamma}. \tag{3.9}$$

The following definition for dimensionless wave speed c_n in the absence of steps will prove useful below:

$$c_n \equiv \frac{(1-\lambda_p)S_t}{\alpha} c_{nd}. \tag{3.10}$$

Among (3.5b), (3.6), (3.8b) and (3.10) it is seen that

$$w_n = c_n S_r. \tag{3.11}$$

3.3. *Cyclic erosional steps of permanent form*

The case of erosional steps is now considered. As outlined in the Introduction, periodic solutions of permanent form migrating upstream with constant wave velocity are sought. The case of interest is illustrated in figure 6, which describes a stepped bed migrating upstream with wave speed c_{sd}, with an additional rate of degradation w_{ad}. That is,

$$\eta_d(x_d, t_d) = \eta_{wd}(x_d + c_{sd}t_d) - w_{ad}t_d. \tag{3.12}$$

It is further assumed that other than this upstream migration and vertical degradation, both at constant rates, neither the bed profile nor the flow changes in time. In general

it is expected that $c_{sd} \neq c_{nd}$. In addition, it is important to realize that w_{ad} is not the total mean degradation rate: another component is realized as the waveform η_{wd} migrates upstream at speed c_{sd}, as explained below. The steps have wavelength L_d and wave height $\Delta\eta_d$, where

$$\Delta\eta_d = \eta_{wd}(x_d) - \eta_{wd}(x_d + L_d). \tag{3.13}$$

In the case of erosional cyclic steps the lack of deposition to balance erosion implies that the mean bed slope S is not determined by the interaction of the flow and sediment, but is rather an antecedent parameter, i.e. equal to the slope S originally prevailing in the absence of steps. Here the Froude number in the absence of steps Fr_n is used as a surrogate parameter for S, which can then be computed from (3.4*a*) once the friction coefficient C_f is specified. As seen from figure 6,

$$S = \frac{\Delta\eta_d}{L_d}. \tag{3.14}$$

The total mean rate of vertical bed degradation w_{sd} in the presence of steps can be determined by averaging (2.3) over one wavelength:

$$w_{sd} = -\overline{\frac{\partial\eta_d}{\partial t_d}} = \frac{\overline{E}}{1-\lambda_p}, \tag{3.15}$$

where the overbar denotes averaging over one wavelength, e.g.

$$\overline{E} = \frac{1}{L_d}\int_{x_d}^{x_d+L_d} E\,\mathrm{d}x_d. \tag{3.16}$$

Again it is expected that $w_{sd} \neq w_{nd}$. Substituting (3.12) into (2.3) and reducing, it is found that

$$-w_{ad} + c_{sd}\frac{\mathrm{d}\eta_{wd}}{\mathrm{d}\tilde{x}_d} = -\frac{E}{1-\lambda_p}, \tag{3.17}$$

where

$$\tilde{x}_d = x_d + c_{sd}t_d. \tag{3.18}$$

Averaging over one wavelength and invoking (3.13)–(3.15) it is found that

$$w_{sd} = c_{sd}S + w_{ad}. \tag{3.19}$$

That is, the total vertical degradation rate is composed of a component $c_{sd}S$ realized in analogy to (3.6) as the waveform sweeps upstream, and an additional component w_{ad} which is independent of wave migration. Here w_{ad} may take negative values as long as the total degradation rate w_{sd} is positive.

In the following analysis the problem will be solved in a spatial coordinate that is moving upstream with constant speed c_{sd}, i.e. the coordinate $\tilde{x}_d$. The tilde is, however, dropped for convenience. Noting that (2.1) is independent of time and therefore invariant to the transformation (3.18), it may be reduced with (2.4) to yield the following ordinary differential equation in the moving coordinate system:

$$u_d\frac{\mathrm{d}u_d}{\mathrm{d}x_d} = -g\frac{\mathrm{d}h_d}{\mathrm{d}x_d} - g\frac{\mathrm{d}\eta_{wd}}{\mathrm{d}x_d} - C_f\frac{u_d^2}{h_d}. \tag{3.20}$$

The dimensionless variables u, h, η and x are introduced at this point in accordance with the following definitions:

$$u_d = u_t u, \quad h_d = \frac{q_w}{u_t}h, \quad \eta_{wd} = \frac{q_w}{u_t}\eta, \quad x_d = \frac{q_w}{u_t S_t}x. \tag{3.21*a–d*}$$

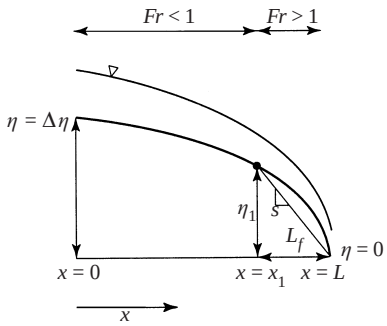

FIGURE 7. Close-up of a single step, showing subcritical and supercritical regimes of flow, the point $x = x_1$ dividing the two regimes and the dimensionless step steepness $s = \eta_1/L_f$.

Note that the parameter S_t has been absorbed into the dimensionless length x, but has not been absorbed into η and h. This has the convenient effect of collapsing the equations into a universal form that is independent of the precise value of S_t. It will be found that such a collapse is no longer possible when geometric nonlinearities become important. Reducing (3.20) with the aid of (2.2), and (3.17) with aid of (3.3), the governing equations reduce to

$$(Fr_t^2 u - u^{-2})\frac{\mathrm{d}u}{\mathrm{d}x} = -\frac{\mathrm{d}\eta}{\mathrm{d}x} - u^3, \tag{3.22}$$

$$c\frac{\mathrm{d}\eta}{\mathrm{d}x} = w_a - (u^2 - 1)^\gamma, \tag{3.23}$$

where the dimensionless wave speed c and additional rate of degradation w_a are given by

$$c = (1 - \lambda_p)S_t\frac{c_{sd}}{\alpha}, \quad w_a = (1 - \lambda_p)\frac{w_{ad}}{\alpha}. \tag{3.24a,b}$$

Eliminating η from (3.22) and (3.23) results in the nonlinear ordinary differential equation

$$\frac{\mathrm{d}u}{\mathrm{d}x} = \frac{c^{-1}[(u^2 - 1)^\gamma - w_a] - u^3}{Fr_t^2 u - u^{-2}}. \tag{3.25}$$

Further progress requires the specification of boundary conditions. For simplicity the origin of the moving coordinate system is taken to be just downstream of a jump, and the bed elevation just beyond the next jump downstream is taken to be zero, as illustrated in figure 7. Reducing with (3.13), this results in the conditions

$$\eta|_{x=0} = \Delta\eta, \quad \eta|_{x=L} = 0, \tag{3.26a,b}$$

where in accordance with (3.21c,d)

$$\Delta\eta = \frac{u_t}{q_w}\Delta\eta_d, \quad L = \frac{u_t S_t}{q_w}L_d. \tag{3.27a,b}$$

The use of the threshold velocity as the scaling in the non-dimensionalization of (3.21a–d) is motivated by the following consideration. In any shallow-water treatment hydraulic jumps are manifested as shocks. In point of fact, however, they have internal structure. The effect of the hydraulic jump is to dissipate energy over a relatively short zone, within which the St. Venant equations do not apply. If by the end of this

relaxation zone the flow velocity has not been reduced to the threshold value for bed erosion, it is reasonable to assume that bed erosion would continue until the threshold value is achieved. In dimensional terms, this implies that u_d should equal u_t just after the relaxation zone. Since in the present analysis the relaxation zone is treated as a shock with vanishing extent, the resulting dimensionless boundary condition on u is

$$u|_{x=0} = 1. \tag{3.28a}$$

Just before the next jump downstream, the velocity must be equal to the conjugate value of the velocity at $x = 0$, resulting in the additional boundary condition

$$u|_{x=L} = \left[\frac{(1 + 8Fr_t^2)^{1/2} - 1}{2}\right]^{-1}. \tag{3.28b}$$

Once (3.25) has been solved, (3.23) may be integrated in accordance with (3.26*a*, *b*) to yield

$$\eta(x) = \frac{1}{c}\int_x^L \left[(u^2 - 1)^\gamma - w_a\right] \mathrm{d}x, \quad \Delta\eta = \frac{1}{c}\int_0^L \left[(u^2 - 1)^\gamma - w_a\right] \mathrm{d}x. \tag{3.29a, b}$$

It is seen from (3.27*a*, *b*) that

$$\frac{\Delta\eta}{L} = \frac{1}{S_t}\frac{\Delta\eta_d}{\Delta L_d}. \tag{3.29c}$$

An equivalent average normal flow in the presence of steps can be delineated according to which (3.4*a*) holds with the further specifications

$$S = \frac{\Delta\eta}{L}, \quad Fr_n^2 = \frac{u_{ed}^3}{g q_w}. \tag{3.30a, b}$$

In the above relations S denotes the mean slope averaged over the steps and u_{ed} denotes the equivalent normal flow velocity satisfying (3.4*a*). In so far as mean bed slope is taken to be an imposed parameter that cannot be changed by the presence of steps, a comparison of (3.4) and (3.30) ensures that $u_{ed} = u_{nd}$. That is, the equivalent normal flow velocity in the presence of steps must be identical to that which would prevail in their absence. The average rate of erosion of the bed in the presence of steps will in general be different from that prevailing in their absence, however, as noted below.

Equation (3.29*b*) can be reduced with the aid of (3.29*c*), (3.30) and (3.7*a*) to yield the following constraint for w_a:

$$w_a = \overline{(u^2 - 1)^\gamma} - c\frac{Fr_n^2}{Fr_t^2}. \tag{3.31}$$

This relation is a dimensionless version of (3.19).

4. Character of the boundary value problem

The first-order ordinary differential equation (3.25) for flow velocity u together with the two boundary conditions (3.28*a*, *b*) and the integral constraint (3.31) presents an interesting system. The friction coefficient C_f must be prescribed as a global parameter. For each set of specified values of threshold velocity for bed erosion u_t, water discharge per unit width q_w and bed slope S, the parameters Fr_t and Fr_n are specified as well. These two Froude numbers are taken as the basic specified

parameters in the present dimensionless formulation. The unknowns are the function $u = u(x)$ and the parameters c, L and w_a. The two boundary conditions and the integral constraint allow, at least in principle, for a determination of the function $u(x)$ and two of the parameters. It would appear, then, that a constraint is missing for a complete solution.

The extra constraint can be obtained by considering the flow field of figure 7. Based on the assumed existence of a hydraulic jump, the upstream portion of the flow regime must be subcritical and the downstream portion supercritical. It follows that there must exist a point $x_1 \in (0, L)$ such that the Froude number Fr defined by the relation

$$Fr^2 \equiv \frac{u_d^3}{g q_w} = Fr_t^2 u^3 \tag{4.1}$$

equals unity. Defining $u_1 \equiv u$ at $x = x_1$, it is seen that the Froude-critical condition is attained when

$$u = u_1 \equiv Fr_t^{-2/3}. \tag{4.2}$$

At this value of u, however, the denominator of the right-hand side of (3.25) vanishes, resulting in an apparent singularity in $\mathrm{d}u/\mathrm{d}x$. If such a singularity were to occur it would render the solution of the problem impossible. A necessary condition to avoid the singularity is, then, that the numerator of (3.25) must vanish as well. This results in an extra compatibility constraint:

$$c = \frac{(u_1^2 - 1)^\gamma - w_a}{u_1^3}. \tag{4.3}$$

It is seen from the above equation and (4.2) that for the physically admissible case $\gamma > 0$, c is positive as long as $Fr_t < 1$ and the following constraint is satisfied:

$$w_a < (u_1^2 - 1)^\gamma = (Fr_t^{-4/3} - 1)^\gamma. \tag{4.4}$$

This justifies the restriction of Fr_t to subcritical values. For a given value of w_a wave speed c is seen to increase as $Fr_t \to 0$ under the constraint $\gamma \geqslant 1.5$. This is consistent with a wave speed that increases in proportion to the intensity of the hydraulic jump.

The specification of (4.3) in itself does not allow solution of the problem. Equation (3.25) now takes the indeterminate form $\mathrm{d}u/\mathrm{d}x = 0/0$ at $x = x_1$. An application of L'Hopital's rule allows the following evaluation:

$$\left.\frac{\mathrm{d}u}{\mathrm{d}x}\right|_{x_1} = u_1^5 \left[\frac{2}{3}\gamma \frac{u_1^2 (u_1^2 - 1)^{\gamma - 1}}{(u_1^2 - 1)^\gamma - w_a} - 1\right]. \tag{4.5}$$

In order to obtain the physically realistic case of a flow that is accelerating from subcritical to supercritical at $x = x_1$, it is necessary that $\mathrm{d}u/\mathrm{d}x|_{x_1}$ be positive. The conditions under which this constraint is satisfied are fairly broad, and include (4.4). They are analysed in more detail below.

5. Numerical solution and results for cyclic steps

The numerical solution of (3.25) and its constraints (3.28) and (3.31) now becomes rather simple. Specifying Fr_n and computing w_a from (3.31) would require an iterative scheme. This is avoided by taking the equivalent but inverse step of specifying w_a and computing Fr_n from (3.31). Equation (3.25) is transformed into a streamwise

coordinate x_s defined to have its origin at the point where critical flow is reached:

$$x_s = x - x_1. \tag{5.1}$$

Using (4.2) and (4.5) to start the integration, (3.25) is integrated in the upstream ($-x_s$) direction until the point $x_s = -L_b$ is reached at which (3.28*a*) is satisfied. Again using (4.2) and (4.5) to start the integration, (3.25) is integrated downstream until the point $x_s = L_a$ is reached at which (3.28*b*) is satisfied. The wavelength L is thus given as

$$L = L_b + L_a. \tag{5.2}$$

The bed profile and wave height are then obtained from (3.29*a, b*).

The integration of (3.25) was carried out using a fourth-order Runge–Kutta scheme. An adaptive scheme was used to shorten the step length in the zone of high velocity just upstream of the hydraulic jump. Equation (3.29*a*) was integrated using the trapezoidal rule.

In performing the numerical analysis the parameter w_a may not be selected arbitrarily. It is, rather, subject to an upper bound w_{au} and a lower bound w_{al}. The upper bound arises from a consideration of (4.5), where it is seen that $\mathrm{d}u/\mathrm{d}x|_{x_1}$ becomes infinite as w_a approaches $(u_1^2-1)^\gamma$ from below. Even larger values of w_a yield negative values of $\mathrm{d}u/\mathrm{d}x|_{x_1}$, which are physically unrealistic in that they imply transition from supercritical to subcritical flow in the downstream direction at the point where the Froude number Fr equals unity. It follows that

$$w_{au} = (u_1^2 - 1)^\gamma \tag{5.3}$$

constitutes an upper bound. It is furthermore apparent from (4.3) that the wave speed c vanishes at this bound.

The lower bound is somewhat less obvious. It consists of the constraint

$$w_{al} = -c. \tag{5.4}$$

The above relation reduces with (4.3) to the form

$$c = -w_a = \frac{(u_1^2 - 1)^\gamma}{u_1^3 - 1}. \tag{5.5}$$

A comparison of (4.3), (5.3) and (5.4) indicates that for any given value of $Fr_t < 1$ (and thus u_1) c takes its maximum value at the lower limit of w_a, and its minimum value of zero at the upper limit of w_a. The lower bound can be demonstrated by substituting the relation

$$w_a = -c(1 + \epsilon) \tag{5.6}$$

into (3.23) and (3.25) and evaluating both at $x = 0$ in accordance with (3.28*a*). Here ϵ is a small parameter which when positive ensures that w_a is below the limit (5.4). The result is

$$\left.\frac{\mathrm{d}\eta}{\mathrm{d}x}\right|_{x=0} = -(1 + \epsilon), \tag{5.7}$$

$$\left.\frac{\mathrm{d}u}{\mathrm{d}x}\right|_{x=0} = -\frac{\epsilon}{1 - Fr_t^2}. \tag{5.8}$$

In the original parameters of the problem before non-dimensionalizing, (5.7) implies a bed slope at $x_d = 0$ that is equal to S_t when $w_a = -c$, and larger than this when $w_a < -c$. According to (3.28*a*), u_d must be equal to u_t at this point. A consideration of the

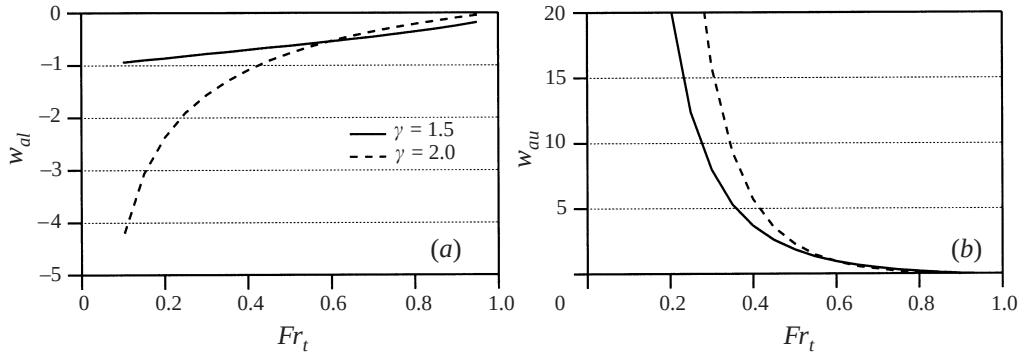

FIGURE 8. (*a*) Lower limit w_{al} on w_a and (*b*) upper limit w_{au} on w_a as a function of Fr_t for the cases $\gamma = 1.5$ and $\gamma = 2$.

physically realistic case of flow that is monotonically accelerating in the downstream direction, however, reveals that an M2 backwater curve computed upstream from the point where $Fr = 1$ cannot reach the condition $u_d = u_t$ at a point where the bed slope is still in excess of S_t. This conclusion is in accordance with (5.8), which indicates that the flow must be decelerating rather than accelerating in the downstream direction at the point $x = 0$ when $w_a < -c$.

It can be shown from the above analysis and a consideration of (4.5) that the constraint $\mathrm{d}u/\mathrm{d}x|_{x_1} > 0$ is satisfied for all values $Fr_t \in (0, 1)$ and $w_a \in [w_{al}, w_{au}]$ as long as $\gamma \geqslant 1.5$. The constraint is also satisfied for $\gamma < 1.5$ over a more restricted range of parameters, such that w_a must exceed w_{al}.

The limits (5.3) and (5.5) are plotted as a function of threshold Froude number Fr_t in figure 8 for the two cases $\gamma = 1.5$ and $\gamma = 2$ in the erosion relation (3.3). As will be seen below, the wavelength L and normal Froude number Fr_n associated with erosional cyclic steps approach the limits 0 and ∞, respectively at the upper limit w_{au} and the corresponding respective limits ∞ and Fr_t at the lower limit w_{al}. The solution domain (Fr_t, Fr_n) for cyclic steps for the case $\gamma \geqslant 1.5$ is thus illustrated in figure 9(*a*). The lower limit is more than a simple mathematical constraint. It will be shown below to have the physical significance of an upstream-migrating solitary step of permanent form.

In the case $\gamma < 1.5$ the solution domain on the (Fr_t, Fr_n)-plane is restricted. This is illustrated in figure 9(*b*) for the cases $\gamma = 1.3$ and 1.0.

In figure 10(*a–c*) the computed wave speed c, additional degradation rate w_a, wavelength L and wave height $\Delta\eta$ are plotted against Fr_n for the respective values of Fr_t of 0.2, 0.4 and 0.6, assuming the value of the exponent γ in the erosion relation to be 1.5. Also shown on the diagrams is the step sharpness s, which is here defined to be given by the relation

$$s = \frac{\eta_1}{L_f}. \tag{5.9}$$

Here η_1 denotes the value of η at $x = x_1$, i.e. where the Froude number attains unity, and L_f denotes the contribution to wavelength L from the part of the waveform downstream of $x = x_1$, i.e. the regime of supercritical flow, as illustrated in figure 7. The same figure illustrates the interpretation of s as a mean bed slope over the domain extending from the point where the Froude-critical condition is reached to the next hydraulic jump downstream. It is, however, a distorted slope consisting of the ratio of a numerator that has been made dimensionless with the length scale q_w/u_t

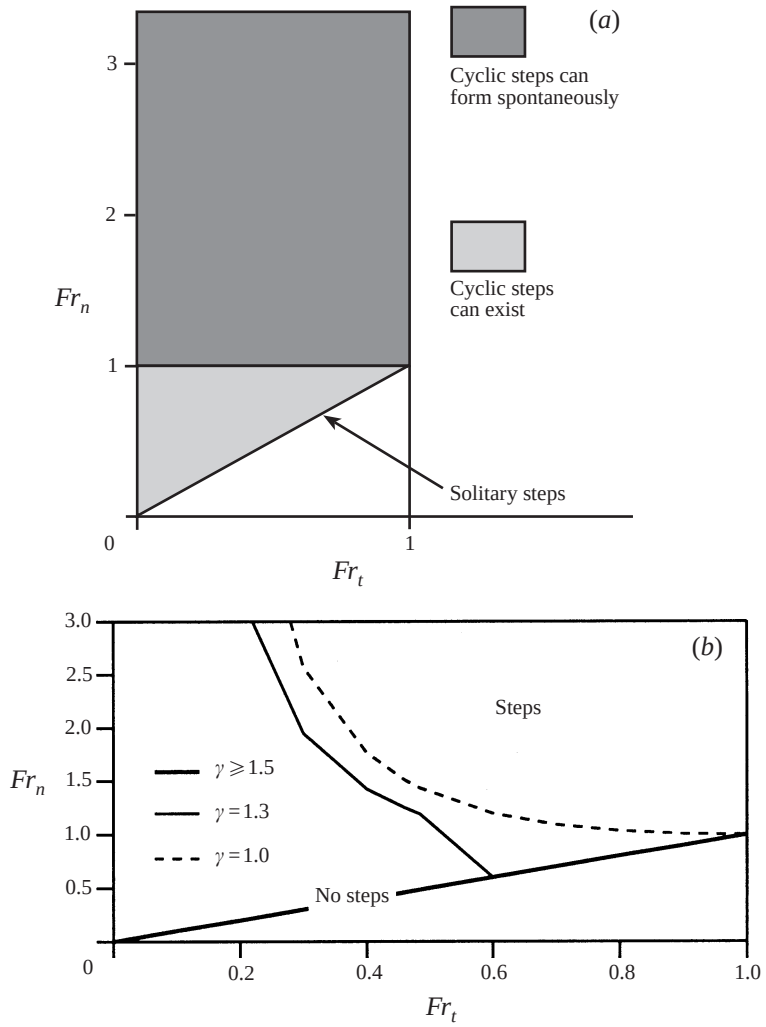

FIGURE 9. (*a*) Fr_n, Fr_t solution domains for cyclic and solitary steps for $\gamma \geqslant 1.5$. (*b*) Modified solution domains for the cases $\gamma = 1.3$ and 1.0.

according to (3.21*c*), and a denominator which has been made dimensionless with the different length scale q_w/u_tS_t in accordance with (3.21*d*). The distortion factor is thus $1/S_t$. The undistorted sharpness s_d (also dimensionless) obtained from the ratio of the two dimensional parameters $\eta_{1d} = (q_w/u_t)\eta_1$ and $L_{fd} = (q_w/u_tS_t)L_f$, i.e.

$$s_d = S_t s \tag{5.10}$$

gives an undistorted mean bed slope over the above-defined domain, i.e. the downstream portion of the step.

Figure 10(*a–c*) indicates that at a set threshold Froude number Fr_t, as Fr_n increases, and thus S increases relative to S_t in accordance with (3.8), c, L and $\Delta\eta$ decrease monotonically and w_a and s increase monotonically. At constant Fr_t, then, larger imposed slopes are thus associated with sharper steps, each with a lower wavelength and wave height, and with a reduced upstream migration speed but increased vertical erosion rate. As indicated by the tendencies in the figures, calculations verify that L

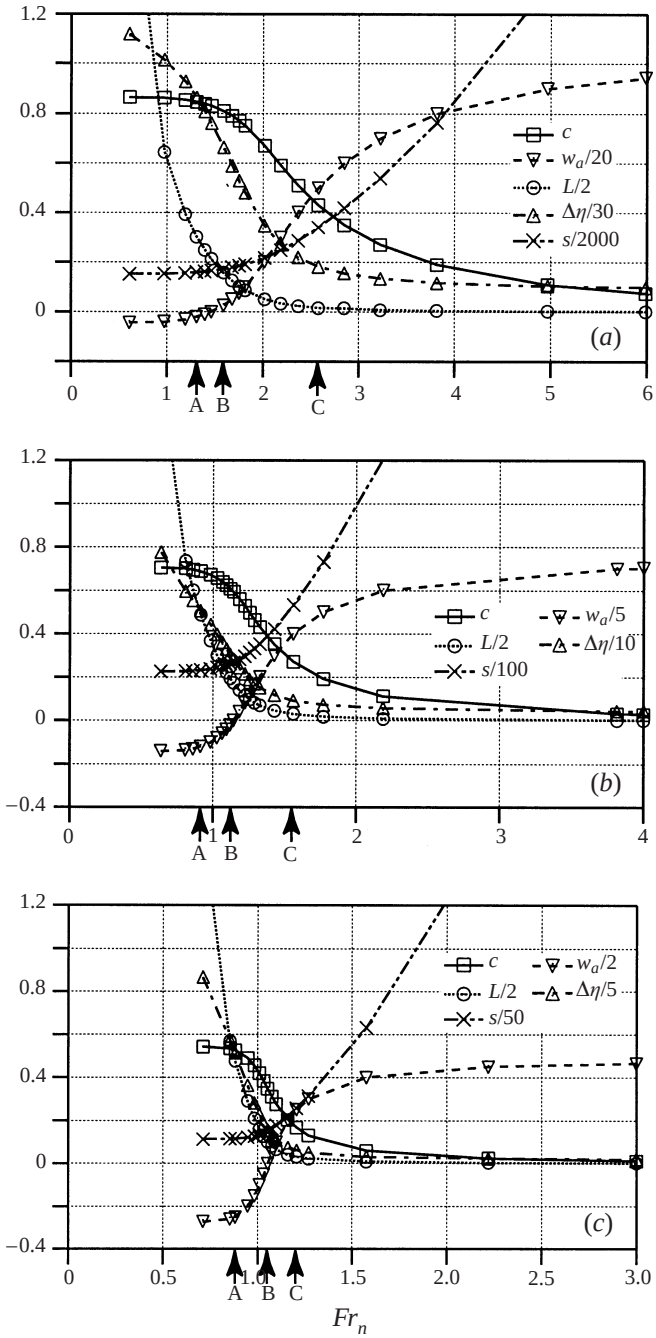

FIGURE 10. Parameters for cyclic steps as functions of Fr_n for the cases (*a*) $Fr_t = 0.2$, (*b*) $Fr_t = 0.4$, (*c*) $Fr_t = 0.6$; $\gamma = 1.5$.

approaches ∞ as Fr_n approaches its lower limit of Fr_t associated with $w_a = w_{al}$, and approaches 0 as Fr_n approaches its upper limit of ∞ associated with $w_a = w_{au}$.

A similar analysis can be performed by holding Fr_n constant and varying Fr_t. As seen from (3.7*b*), increasing Fr_t corresponds to increasing the threshold flow velocity

Fr_t	γ	Fr_n	w_a	c	L	$\Delta\eta$	s	w	c_r	w_r
0.2	1.5	1.191	−0.60	0.854	0.786	27.84	313	29.7	0.988	0.968
0.2	1.5	1.463	0	0.830	0.426	22.81	331	44.4	0.926	0.926
0.2	1.5	2.369	8.00	0.510	0.047	6.55	575	79.6	0.540	0.600
0.2	2.0	1.191	4.90	2.048	0.123	4.37	543	78.8	0.770	0.821
0.2	2.0	1.463	10.29	1.868	0.075	4.03	638	110.2	0.574	0.633
0.2	2.0	2.369	28.28	1.149	0.024	3.34	1177	188.2	0.238	0.280
0.4	1.5	0.912	−0.60	0.688	0.973	5.059	23.2	2.98	1.264	1.052
0.4	1.5	1.142	0	0.593	0.346	2.815	26.8	4.83	0.907	0.907
0.4	1.5	1.559	2.00	0.272	0.061	0.919	53.2	6.13	0.356	0.528
0.4	2.0	0.912	−0.295	0.963	0.281	1.460	36.3	4.71	1.251	1.118
0.4	2.0	1.142	1.07	0.745	0.124	1.010	47.4	7.14	0.653	0.768
0.4	2.0	1.559	3.18	0.407	0.043	0.658	86.2	9.36	0.235	0.355
0.6	1.5	0.881	−0.50	0.527	0.953	2.056	5.77	0.636	2.074	1.162
0.6	1.5	1.054	0	0.347	0.201	0.622	7.56	1.071	0.904	0.904
0.6	1.5	1.206	0.50	0.167	0.061	0.247	12.9	1.175	0.355	0.618
0.6	2.0	0.881	−0.368	0.475	0.344	0.742	7.90	0.656	2.291	1.468
0.6	2.0	1.054	0.176	0.280	0.099	0.304	11.95	1.040	0.688	0.829
0.6	2.0	1.206	0.501	0.163	0.045	0.184	18.89	1.159	0.278	0.490

TABLE 2. Some characteristic parameters of cyclic steps for the cases $Fr_t = 0.2$, 0.4, 0.6 and $\gamma = 1.5$, 2.0.

u_t or decreasing the water discharge per unit width q_w. Over the domain of calculation of figure 10(*a–c*), c, L and $\Delta\eta$ again decrease monotonically and w_a again increases monotonically. The steepness s, however, decreases in Fr_t. This implies that for a given slope S, and water discharge per unit width q_w, increased values of the critical velocity u_t correspond to more gentle steps, each with a lowered migration speed, wavelength and wave height. It is apparent from the above that the sharpest steps are associated with low values of Fr_t, which cause stronger hydraulic jumps, and high values of Fr_n, which cause higher rates of erosion. This latter aspect can be quantified in terms of a dimensionless total degradation rate w in the presence of steps, where in analogy to (3.24*b*)

$$w = (1 - \lambda_p)\frac{w_{sd}}{\alpha}. \tag{5.11}$$

Reducing (3.31) with (3.19), (3.24) and (5.11), it is found that

$$w = c\frac{Fr_n^2}{Fr_t^2} + w_a. \tag{5.12}$$

The value of w is found to increase with increasing Fr_n. This can be readily seen from table 2, which is explained in more detail below.

In order to obtain a view of the variation of step shape with the parameters Fr_t, and Fr_n for the case $\gamma = 1.5$, a total of nine cases were considered, as shown in table 2. Three calculations were performed at each of the threshold Froude numbers Fr_t of 0.2, 0.4 and 0.6. For each Froude number calculations were performed using a negative value of w_a, $w_a = 0$ and a positive value of w_a. The respective cases are marked on figure 10(*a–c*) as A, B and C. The resulting dimensionless bed and water surface profiles are shown in figure 11(*a–i*). Dimensional water surface elevation ξ_d

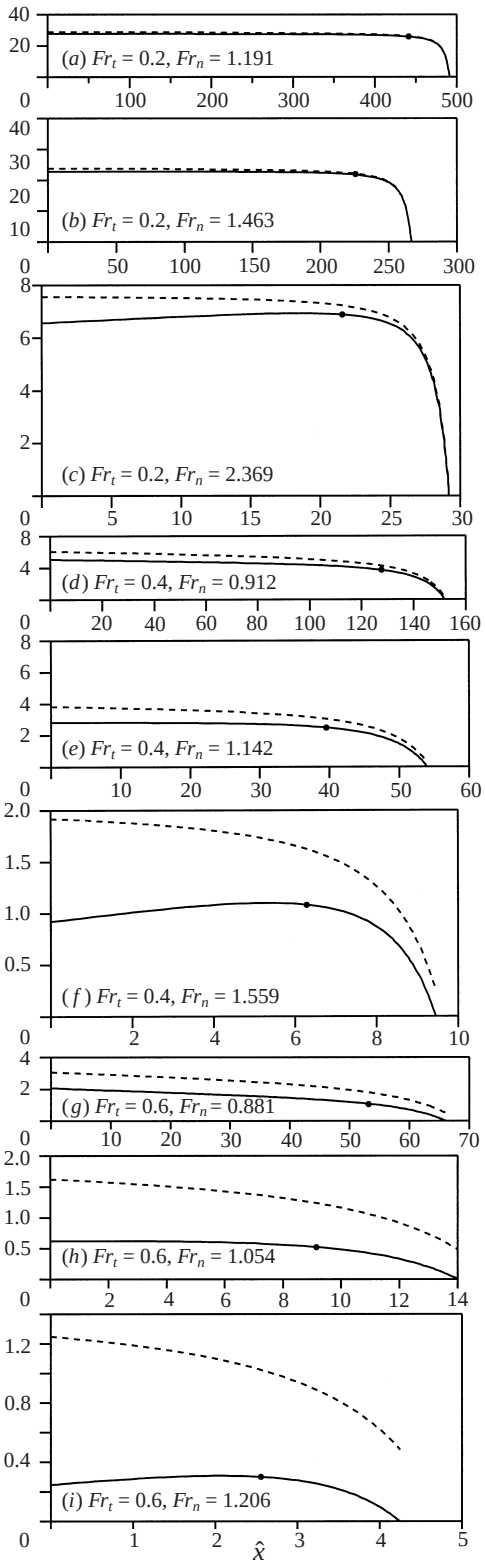

FIGURE 11. For caption see facing page.

is given by the relation

$$\xi_d = \eta_d + h_d = \eta_d + \frac{q_w}{u_d}. \tag{5.13a}$$

The corresponding dimensionless form is

$$\xi = \frac{u_t}{q_w}\xi_d = \eta + u^{-1}. \tag{5.13b}$$

As mentioned above, the differing non-dimensionalizations associated with (3.21*c*) and (3.21*d*) imply that plots of η and ξ versus x have an inherent distortion. In order to remove the effect of this distortion from the plots, η and ξ have been plotted versus the dimensionless distance $\hat{x}$, where

$$\hat{x} = \frac{x}{S_t} = \frac{u_t}{q_w}x_d. \tag{5.14}$$

The values of $\hat{x}$ used in the plots were computed for the case $C_f = 0.04$, yielding values of S_t of 0.0016. 0.0064 and 0.0144 for the respective cases $Fr_t = 0.2$, 0.4 and 0.6 according to (3.7*a*).

In figure 11(*a–i*), the plotted vertical scale was distorted by a factor of approximately 2 for clarity. The point on the bed at which Froude-critical conditions are reached is marked on each plot. As expected, the sharpest step is realized for the smallest value of Fr_t and the largest value of Fr_n. The three cases for which $w_a = 0$ correspond to a bed slope that is vanishing at the upstream end. This implies pure wave translation without any additional degradation. The three cases corresponding to negative values of w_a have positive bed slopes at the upstream end; here the degradation associated with pure wave translation is ameliorated by the negative value of w_a. The three cases corresponding to positive values of w_a have adverse bed slopes at the upstream end. As illustrated in figure 12, the highest adverse bed slope that can be preserved as the bed degrades is given by the dimensional condition $w_{ad} = -S_l c_{sd}$, where $S_l(< 0)$ denotes a local adverse bed slope. This criterion takes the dimensionless form

$$-S_{lr} \equiv -\frac{S_l}{S_t} = \frac{\mathrm{d}\eta}{\mathrm{d}x} = \frac{w_a}{c}. \tag{5.15}$$

It is immediately seen from (3.23), (3.25) and (3.28*a*) that the local adverse bed slope of the highest magnitude that can be realized is at the upstream end, where

$$\left.\frac{\mathrm{d}\eta}{\mathrm{d}x}\right|_{x=0} = \frac{w_a}{c}. \tag{5.16}$$

Between (5.15) and (5.16), then, it is seen that the criterion for preservation of an adverse slope is inherently satisfied by the solution.

Also shown in table 2 are the results of similar calculations for the case $\gamma = 2$ in the erosion relation (3.3). In order to allow a direct comparison, the calculations for the case $\gamma = 2$ correspond the same values of (Fr_t, Fr_n) as those for the case $\gamma = 1.5$. As a result, the values of w_a differ between the two cases. For the same values of (Fr_t, Fr_n), an increased erosion exponent is seen to result in higher values of w_a and s, and lower values of L and $\Delta\eta$. The values of c are increased for the cases $Fr_t = 0.2$

FIGURE 11. Bed (η, solid line) and water surface (ξ, dashed line) profiles of a single cyclic step for $\gamma = 1.5$ and the indicated values of Fr_t and Fr_n. The dot on the bed denotes the point at which a Froude number of unity is attained.

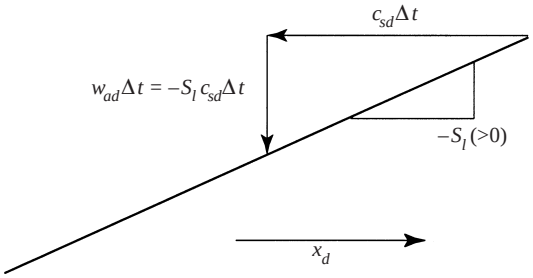

FIGURE 12. Condition for the preservation of adverse slope.

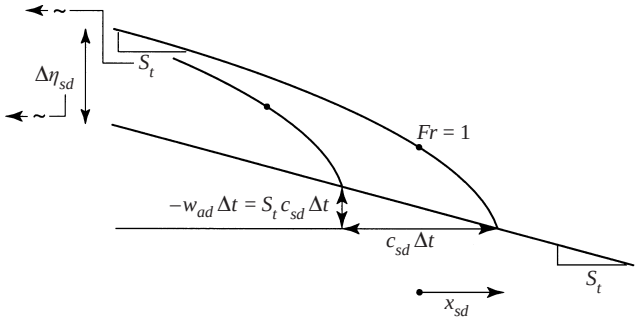

FIGURE 13. Diagram showing the conditions under which a solitary step migrates upstream without changing form.

and 0.4, but decreased for the case $Fr_t = 0.6$. An increase in γ from 1.5 to 2 thus yields steps that are shorter and lower, but steeper over the range investigated.

6. The solitary step

The above theory for cyclic steps allows a solution for a self-preserving solitary step of permanent form as a limiting case. On physical grounds, the conditions for the existence of such a step are illustrated in figure 13. The bed slope immediately downstream of the step must be S_t, and this value must be continued infinitely far downstream. This corresponds to a value of $\mathrm{d}\eta/\mathrm{d}x$ of -1. Likewise, the bed slope converges to the value S_t far upstream. In order that the form be preserved as it migrates upstream with speed c_{sd}, the additional bed degradation rate w_{ad} must be negative, and precisely equal to $S_t c_{sd}$. In dimensionless terms, this corresponds to the condition (5.4), i.e. the lower bound on w_a for the formation of cyclic steps.

Figure 10(*a–c*) suggests that the wavelength L approaches infinity as the lower limit in w_a is approached. That this is indeed true as long as $\gamma > 1$ is demonstrated below. At the limiting value (5.4), (3.25) can be rewritten with (5.4) and (5.5) to yield

$$\frac{\mathrm{d}u}{\mathrm{d}x} = \frac{\dfrac{(u^2-1)^\gamma}{(u_1^2-1)^\gamma}(u_1^3-1)+1-u^3}{Fr_t^2 u - u^{-2}}. \tag{6.1}$$

Now let $\Delta x(\epsilon)$ denote the distance from the point where $u = 1$ is realized, i.e. the upstream boundary, to a point slightly downstream where $u = 1 + \epsilon$, ϵ being a small

positive number. Taylor-expanding and integrating (6.1), it is found that

$$\Delta x(\epsilon) = \frac{1}{1 - Fr_t^2} \int_0^{\epsilon} \frac{1}{3\epsilon - R\epsilon^{\gamma}} \mathrm{d}\epsilon, \quad R = 2\gamma \frac{u_1^3 - 1}{(u_1^2 - 1)^{\gamma}} 2^{\gamma}. \tag{6.2}$$

It is readily seen that $\Delta x(\epsilon) \to \infty$ as $\epsilon \to 0$ under the constraint $\gamma > 1$.

The fact that L converges to infinity in the case of solitary steps renders several of the previous definitions for cyclic steps meaningless for solitary steps. Since the boundary condition (3.28*a*) is now satisfied as an asymptote infinitely far upstream, it is appropriate to redefine the coordinate system in terms of the parameter x_s defined by (5.1), the origin of which corresponds to the point where Froude-critical conditions are reached. That is, (3.28*a*) now becomes

$$\lim_{x_s \to -\infty} u(x_s) = 1. \tag{6.3}$$

It is seen from figure 13 that step height $\Delta\eta$ is now given by

$$\Delta\eta = \lim_{x_s \to -\infty} \eta(x_s) = \infty. \tag{6.4}$$

If the step height $\Delta\eta_s$ appropriate for solitary steps is defined as follows, however, the limit is found to converge:

$$\Delta\eta_s = \lim_{x_s \to -\infty} [\eta(x_s) + x_s]. \tag{6.5}$$

The corresponding dimensional wave height is then $\Delta\eta_{ds} = (q_w/u_t)\Delta\eta_d$ in accordance with (3.27*a*). From (3.30*a, b*), (5.2) and (6.5), then,

$$S_r = \lim_{x_s \to -\infty} \frac{\eta(x_s)}{L_f - x_s} = \lim_{x_s \to -\infty} \frac{[\eta(x_s) + x_s] - x_s}{L_f - x_s} = 1. \tag{6.6}$$

It follows from (3.8*b*) that the case of solitary steps corresponds to the condition

$$Fr_n = Fr_t, \tag{6.7}$$

as illustrated in the domain diagram of figure 9(*a*) for the case $\gamma \geqslant 1.5$. It is furthermore seen from the above equation, (5.4) and (5.12) that

$$w = 0. \tag{6.8}$$

That is, the negative value of w_a perfectly compensates for the degradation inherent in the translation of the waveform upstream at speed c, resulting in preservation of form.

In figure 14(*a–c*) the parameters c, $\Delta\eta_s$ and s_s are plotted against Fr_t for the case of solitary steps. Here s_s is a steepness appropriate for solitary steps, defined as

$$s_s = \frac{\eta_1 - L_f}{L_f}. \tag{6.9a}$$

In analogy to (5.10), this can be converted to an undistorted steepness s_{sd} by means of the relation

$$s_{sd} = S_t s_s. \tag{6.9b}$$

Results in the figure are presented for both the cases $\gamma = 1.5$ and $\gamma = 2$. It is seen that wave speed c, wave height $\Delta\eta_s$ and steepness s_s all decrease with increasing Fr_t. In the case of the last two parameters, the decrease is sufficiently precipitous to necessitate a logarithmic scale. As expected, the steps are progressively more well defined as Fr_t becomes small.

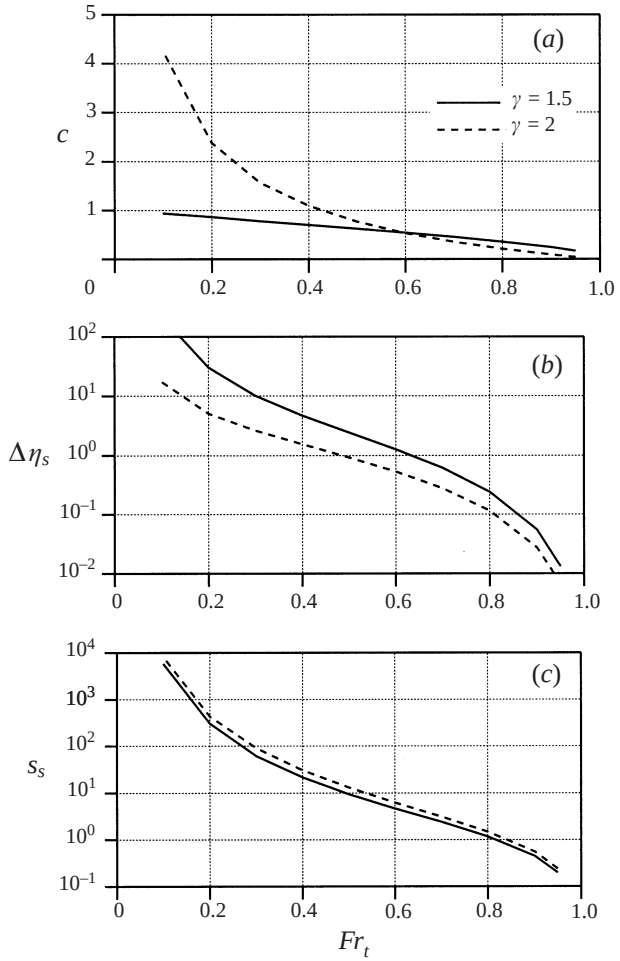

FIGURE 14. (*a*) Dimensionless upstream wave speed of solitary steps c, (*b*) dimensionless wave height of solitary steps $\Delta\eta_s$, (*c*) dimensionless wave steepness of solitary steps s_s, as functions of Fr_t for the cases $\gamma = 1.5$ and $\gamma = 2$.

In figure 15(*a–c*) profiles for solitary steps are plotted for the cases $Fr_t = 0.2$, 0.4 and 0.6, respectively, with $\gamma = 1.5$. The associated parameters are given in table 3. The plots have been constructed so as to show all of the step downstream of the point where Froude-critical conditions are reached, as well as an upstream portion of equal length. In analogy to (5.14), the distortion inherent in plotting η and ξ against x is removed by plotting them against $\hat{x}_s$ instead, where

$$\hat{x}_s = \frac{x_s + L_f}{S_t}. \tag{6.10}$$

This transformation places the origin of the coordinate system at the upstream end of the reach that is actually plotted. Otherwise the plots conform to the conventions of figure 11(*a–i*). The tendency for $\Delta\eta_s$ and s_s to increase as Fr_t decreases is readily apparent from the figure.

Table 3 also includes the results of calculations of solitary steps with $\gamma = 2.0$. It can be seen there that an increase in γ from 1.5 to 2.0 results in a decrease in step height

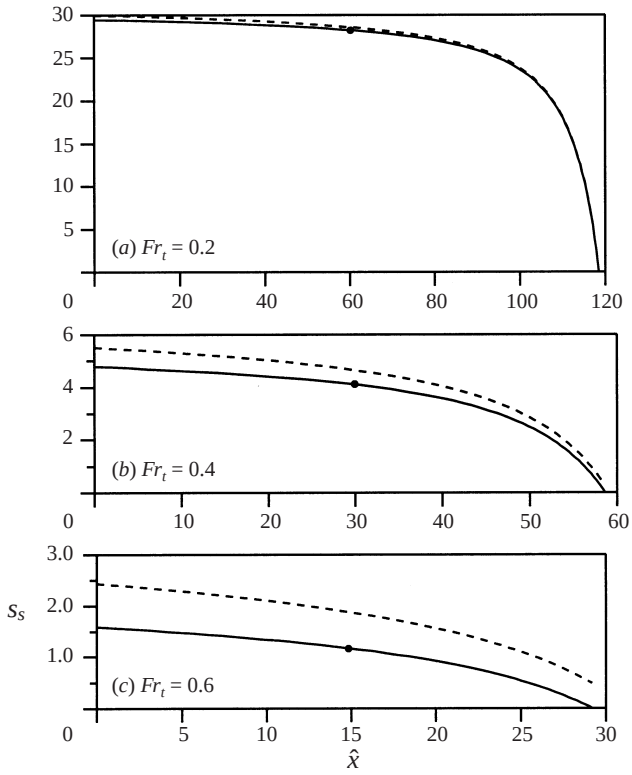

FIGURE 15. Bed (η, solid line) and water surface (ξ, dashed line) profiles of a solitary step for $\gamma = 1.5$ and the indicated value of Fr_t. The dot on the bed denotes the point at which a Froude number of unity is attained.

Fr_t	γ	$c\,(= w_a)$	$\Delta\eta_s$	s_s
0.2	1.5	0.864	29.97	303
0.2	2.0	2.375	5.06	438
0.4	1.5	0.705	4.65	21.5
0.4	2.0	1.091	1.54	30.7
0.6	1.5	0.542	1.255	4.66
0.6	2.0	0.536	0.532	6.22

TABLE 3. Some characteristic parameters of solitary steps for the cases $Fr_t = 0.2$, 0.4, 0.6 and $\gamma = 1.5$, 2.0.

$\Delta\eta_s$ and an increase in step sharpness s_s. Wave speed c is increased for the Froude numbers $Fr_t = 0.2$ and 0.4, but is reduced in the case $Fr_t = 0.6$.

In the present analysis the case describing solitary steps has been obtained as a limiting case of cyclic steps each one of which is bounded by points where the threshold velocity for bed erosion is attained. This constrains the solution to one that attains a constant, uniform velocity equal to the threshold value for bed erosion over a bed at the constant slope S_t far upstream. It is shown in Izumi & Parker (2000), however, that solutions for solitary steps can be obtained under a much wider range

of conditions, including those for which the flow velocity is either below or above the threshold of erosion far upstream.

7. Conditions for the spontaneous development of steps

The above analysis of cyclic and solitary steps considers finite-amplitude solutions of permanent form. It does not address the question as to whether or not a flow able to erode a flat bed without steps will spontaneously devolve into a flow over a stepped bed. An appropriate means for addressing this question is linear stability analysis. To this end, the normal flow over a bed with slope $S > S_t$ is considered. The normal solution of (3.4) and (3.5) is then slightly perturbed to see if imposed bed undulations will grow or die. The analysis below is in fact very similar to that presented by Sawai (1977).

In dimensional terms, the flow velocity and bed profile are represented as

$$u_d = u_{nd} + u_{pd}, \quad \eta_d = \eta_{rd} - Sx_d - w_{nd}t_d + \eta_{pd}. \tag{7.1a,b}$$

Here u_{nd} and w_{nd} are given by (3.4b) and (3.5a), respectively; η_{rd} is a reference bed elevation at the point $(x_d, t_d) = (0, 0)$ and u_{pd} and η_{pd} represent slight perturbations about the normal state. Equations (7.1a,b) are now substituted into (2.1) and (2.3), reduced with (2.2) and (3.3), Taylor-expanded to the linear level in the terms u_{pd} and η_{pd}, and made dimensionless in accordance with the following scheme, which is similar to (3.21) but based on u_{nd} rather than u_t:

$$u_{pd} = u_{nd}u_p, \quad \eta_{pd} = \frac{q_w}{u_{nd}}\eta_p, \tag{7.2a,b}$$

$$x_d = \frac{q_w}{u_{nd}S_t}x, \quad t_d = \frac{\alpha}{(1-\lambda_p)\dfrac{q_w}{u_{nd}}}t. \tag{7.2c,d}$$

The parameter x defined above is similar but not identical to that defined in (3.21d). Rather than allow notation to proliferate, it is understood here that the above definition is used in this section only. The resulting linearized versions of (2.1) and (2.3) are

$$(Fr_n^2 - 1)\frac{\partial u_p}{\partial x} = -\frac{\partial \eta_p}{\partial x} - 3u_p, \tag{7.3}$$

$$\frac{\partial \eta_p}{\partial t} = -Qu_p, \quad Q = 2\gamma u_n^2(u_n^2 - 1)^{\gamma-1}. \tag{7.4a,b}$$

Sinusoidal perturbations with wavenumber k and complex wave celerity c_p made dimensionless in accordance with (7.2) are introduced as follows:

$$\eta_p = \eta_* e^{ik(x-c_p t)}, \quad u_p = u_* e^{ik(x-c_p t)}. \tag{7.5a,b}$$

It is important to realize that the complex wave celerity c_p differs from the upstream wave speed c of the above analysis in several ways. The celerity c_p is a dimensionless quantity formed from the scales of (7.2) rather than (3.21). It is composed of a real part c_{pr} and an imaginary part c_{pi}, where c_{pr} corresponds to the wave speed and kc_{pi} corresponds to the growth rate of the perturbation. A positive value of c_{pr} corresponds to perturbations that migrate in the downstream direction. Substituting (7.5a,b) into

(7.3) and (7.4) and reducing, it is found that

$$c_{pr} = -3\frac{Q}{k^2(Fr_n^2-1)^2+9}, \quad c_{pi} = \mathrm{i}k\left(Fr_n^2-1\right)\frac{Q}{k^2(Fr_n^2-1)^2+9}. \tag{7.6a,b}$$

In so far as $Q > 0$ for any positive value of γ under the condition $u_n > 1$ considered here, the following results hold. The migration speed c_{pr} is negative for all wavenumbers k and normal Froude numbers Fr_n, corresponding to upstream migration. The growth rate kc_{pi} of the perturbation, however, is seen to be positive only when $Fr_n > 1$, i.e. when the normal flow is supercritical. That is, upstream-migrating erosional forms that might evolve into cyclic steps form spontaneously only under conditions of supercritical flow. The regime where the spontaneous formation of steps might be expected is denoted in figure 9(*a*) for the case $\gamma \geqslant 1.5$. The above result does not imply that cyclic steps (or their solitary limit) will not form for subcritical normal flows. Rather, it implies that a finite-amplitude perturbation is probably necessary to start their formation.

The infinitesimal bedforms predicted by the above stability analysis are such that the water surface is approximately in phase with the bed under the condition that $Fr_n > 1$. They are thus seen to correspond to the purely erosional analogue of antidunes associated with sediment suspended over a non-cohesive bed. These antidunes have been studied by such researchers as Kennedy (1963), Engelund (1970), and Fredsoe (1974). None of these used the long-wave, or slender-flow approximation to formulate the problem. Their work demonstrates that the Froude number for critical flow conditions is in fact wavenumber dependent. For long waves, the Froude-critical condition is indeed $Fr = 1$, but for shorter waves the critical condition drops substantially below unity. It is for this reason that antidunes often form in flow that is subcritical to long waves. The present analysis, then, applies only to long-wave phenomena. Both short-wave erosional antidunes and cyclic steps may exist; the present analysis sheds no light as to how the former forms and whether or not it evolves into the latter.

8. Discussion

It is of value to compare the wave speeds and vertical degradation rates in the presence of erosional steps with those in their absence. To this end the following ratios are defined:

$$c_r = \frac{c}{c_n}, \quad w_r = \frac{w}{w_n}, \tag{8.1a,b}$$

where w is defined as

$$w \equiv \frac{(1-\lambda_p)w_{sd}}{\alpha}. \tag{8.2}$$

That is, c_r and w_r respectively denote the ratio of wave speed and total degradation rate, with and without steps. Among (3.3), (3.8*a*), (3.9), (3.11), (3.15), (3.31) and the definitions (3.24*b*) and (8.2) it is found that

$$w_r = \frac{\overline{(u^2-1)^\gamma}}{(u_n^2-1)^\gamma} = \frac{c\left(Fr_n/Fr_t\right)^2 + w_a}{\left[\left(Fr_n/Fr_t\right)^{4/3}-1\right]^\gamma}, \quad c_r = \frac{c\left(Fr_n/Fr_t\right)^2}{\left[\left(Fr_n/Fr_t\right)^{4/3}-1\right]^\gamma}. \tag{8.3a,b}$$

Values for w_r and c_r are shown in table 2. Of interest is the observation that either of these parameters can be greater or less than unity. That is, the degradation or

upstream migration rate in the presence of steps may be greater or less than the value prevailing in the absence of steps, depending upon imposed conditions.

The fundamental nonlinearity of the erosion law (3.3) implies that any deviation due to the presence of steps from the constant normal velocity u_n that would prevail in the absence of steps should act to increase the reach-averaged erosion rate. Such an increase is indeed observed for relatively large values of Fr_t and relatively small values of Fr_n, as can be seen from table 3. In the region where Fr_t is small and Fr_n is large, which also corresponds with the most well-developed steps, it is seen on the other hand that the steps act to suppress the erosion rate rather than enhance it.

The reason for this is related to another fundamentally nonlinear phenomenon, the hydraulic jump defining each step. To see this, (3.8*a*) and (3.31) are used to recast (3.25) into the following form:

$$\frac{\mathrm{d}E_s}{\mathrm{d}x} = S_r + \frac{(u^2-1)^\gamma - \overline{(u^2-1)^\gamma}}{c} - u^3. \tag{8.4}$$

Here E_s denotes a dimensionless specific energy, given by the relation

$$E_s = \tfrac{1}{2}Fr_t^2 u^2 + u^{-1}. \tag{8.5}$$

Integrating (8.4) from $x = 0$ to $x = L$ under the constraints (3.28*a*, *b*) yields the relation

$$\overline{u^3} = S_r - \frac{\Delta E_s}{L}, \tag{8.6}$$

where ΔE_s is a positive quantity that denotes the energy loss through the jump, given by

$$\Delta E_s = \tfrac{1}{2}Fr_t^2\left(u_{con}^2 - 1\right) + \left(u_{con}^{-1} - 1\right), \quad u_{con} = \left[\frac{(1+8Fr_t^2)^{1/2}-1}{2}\right]^{-1}. \tag{8.7a, b}$$

Equation (8.6) can now be readily interpreted in terms of classical open channel hydraulics. The parameter $\overline{u^3}$ is a dimensionless version of the mean friction slope, and S_r likewise denotes a dimensionless mean bed slope. In the absence of steps, and thus the associated hydraulic jumps, the mean friction slope would equal the mean bed slope. In the presence of steps, however, $\overline{u^3}$ must drop below S_r by an amount corresponding to the energy loss per unit distance associated with each hydraulic jump. As Fr_t becomes small the intensity of the hydraulic jump increases, causing ΔE_s to increase. It was likewise seen earlier that L approaches 0 as Fr_n becomes large. Thus small values of Fr_t and large values of Fr_n imply decreased values of $\overline{u^3}$, and thus a decreased rate of erosion of the bed in the presence of steps.

The above comments are not meant to imply that the hydraulic jump plays no role in the erosion process. The boundary condition (3.28*a*) is based on the assumption that erosion at the base of the step continues as cyclic steps develop until the threshold condition is attained. Cyclic steps of permanent form are thus assumed to be the end product of this development process.

The conclusion that the average erosion rate in the presence of steps is lower that in their absence when Fr_t is small and Fr_n is large may have some useful practical implications as regards erosion control.

The issue of the boundary condition (3.28*a*) deserves more attention. A reanalysis of the problem indicates that the boundary condition

$$u|_{x=0} = u_s, \quad 1 < u_s < \min\left(Fr_t^{-2/3}, u_n\right) \tag{8.8}$$

also results in solutions for cyclic steps. The upper bounds result from the following considerations. A Froude number Fr_s may be defined such that

$$Fr_s^2 = u_s^3 Fr_t^2. \tag{8.9}$$

Two necessary conditions for the formation of cyclic steps are that $Fr_s < 1$ and $Fr_s < Fr_n$. This can be seen by substituting Fr_s for Fr_t in figure 9(*a*). One of these conditions combined with (8.9) results in the first bound in (8.8); the other combined with (3.8*a*) results in the second one.

It is suggested here that solutions for cyclic steps satisfying (8.8) may represent an unstable finite-amplitude equilibrium. That is, any small perturbation would result in the initiation of scour at the toe of each step, which would then only be completely stabilized when the threshold condition for bed erosion is attained just beyond the hydraulic jump, i.e. when (3.28*a*) is satisfied. A proper resolution of this question would require a full nonlinear stability analysis. This technique has provided extremely useful results as regards other erodible-bed problems (e.g. Colombini, Seminara & Tubino 1987; Schielen, Doelman & Swaart 1993). It is, however, beyond the scope of the present analysis.

As pointed out in the introduction, cyclic steps need not be purely erosional. Winterwerp *et al.* (1992) have observed virtually the same phenomenon in non-cohesive fine sediment under conditions for which there is no net erosion of the bed; these are here termed transportational cyclic steps. These are probably different manifestations of the same underlying mechanism. In addition, it may be that the step–pool topography characteristic of steep gravel-bed streams (e.g. Whittaker & Jaeggi 1982; Ashida, Egashira & Nishimoto 1986; Grant & Mizuyama 1991) is a somewhat more distantly related phenomenon.

A final point concerns the long-wave approximation. The calculations presented here show that wavelength L converges to 0 as Fr_n approaches infinity. The long-wave approximation ceases to hold in this limit; the results are nevertheless shown in order to show the general behaviour of the theory. The present theory does not apply whenever the predicted ratio of characteristic depth to wavelength ceases to be small.

9. Finite-slope generalization

While the forms (2.1)–(2.3) can be expected to be accurate as long as the bed slope is not too high, their application to cases for which the slope angle exceeds more than a few degrees becomes suspect. Consider, for example, the case corresponding to $\gamma = 1.5$, $Fr_t = 0.2$ and $Fr_n = 1.191$ of table 2, for which the step steepness s defined in (5.9) is 313. Between (3.7*a*) and (5.10) it is found that the average bed slope s_d from the Froude-critical point to just before the hydraulic jump and the corresponding slope angle θ_f are given by the relations

$$s_d = C_f Fr_t^2 s, \quad \theta_f = \tan^{-1}(s_d). \tag{9.1a, b}$$

In the case of a friction coefficient C_f of 0.001, it is found that θ_f is equal to 0.72°, a value low enough to justify the neglect of geometric nonlinearities. When $C_f = 0.05$, however, the value of θ_f increases to 32.0°, a value at which such nonlinearities can be expected to be important.

With this in mind, the forms (2.1) and (2.3) appropriate for an infinitesimal-slope

analysis are generalized below to their finite-slope forms:

$$\frac{\partial u_d^2 h_d}{\partial s_d} = g h_d \sin\theta - \frac{1}{2} g \frac{\partial}{\partial s_d} h_d^2 \cos\theta - \frac{\tau_b}{\rho}, \tag{9.2}$$

$$\cos\theta (1-\lambda_p) \frac{\partial \eta_d}{\partial t_d} = -E, \tag{9.3}$$

where s_d denotes a boundary-attached downslope streamwise coordinate tangent to the bed, h_d now denotes depth normal to the bed and x_d, s_d, η_d and bed angle θ are related as

$$\frac{\partial x_d}{\partial s_d} = \cos\theta, \quad \frac{\partial \eta_d}{\partial s_d} = -\sin\theta. \tag{9.4a,b}$$

As long as the bed curvature is not too large the following approximation is accurate:

$$\frac{1}{2}\frac{\partial}{\partial s_d} h_d^2 \cos\theta = h_d \cos\theta \frac{\partial h_d}{\partial s_d} - \frac{1}{2} h_d^2 \sin\theta \frac{\partial \theta}{\partial s_d} \approx h_d \cos\theta \frac{\partial h_d}{\partial s_d}. \tag{9.5}$$

Equations (9.2) and (9.3) are now reduced with (2.2), (2.4), (9.4), (9.5) and (3.12) and rendered dimensionless in accordance with (3.21) and (3.24), with the exceptions that (3.21d) and (3.24a) are generalized to the respective forms

$$x_d = \frac{q_w}{u_t \sin\theta_t} x, \quad c = (1-\lambda_p) \sin\theta_t \frac{c_{sd}}{\alpha}. \tag{9.6a,b}$$

In the above relations the angle θ_t corresponding to the threshold for erosion at normal conditions is given by the finite-slope generalization of (3.7a):

$$\sin\theta_t = C_f Fr_t^2. \tag{9.7}$$

This results in the following finite-slope generalizations of (3.23) and (3.25), respectively:

$$c \frac{\sin\theta}{\sin\theta_t} + w_a \cos\theta = (u^2-1)^\gamma, \tag{9.8}$$

$$\frac{\mathrm{d}u}{\mathrm{d}x} = \frac{\sin\theta/\sin\theta_t - u^3}{(Fr_t^2 u - u^{-2}\cos\theta)\cos\theta}. \tag{9.9}$$

A consideration of Froude-critical conditions leads to the following generalizations of (4.2) and (4.3):

$$u_1 = Fr_t^{-2/3} \cos^{1/3}\theta_1, \quad \tan\theta_1 = C_f, \tag{9.10a,b}$$

$$c = \frac{\left(u_1^2-1\right)^\gamma - w_a \cos\theta_1}{u_1^3}, \tag{9.11}$$

where θ_1 denotes the bed slope angle at the Froude-critical point. The finite-slope generalizations of (3.4a), (3.31), (4.5), (5.3) and (5.4) are found to be

$$\sin\theta_n = C_f Fr_n^2, \quad \tan\theta_n = S, \tag{9.12a,b}$$

$$w_a = \overline{\left[\frac{(u^2-1)^\gamma}{\cos\theta}\right]} - \frac{c}{\cos\theta_n}\frac{Fr_n^2}{Fr_t^2}, \tag{9.13}$$

$$\left.\frac{\mathrm{d}u}{\mathrm{d}x}\right|_{x_1} = u_1^5 \frac{\left\{\frac{2}{3}\gamma[u_1^2(u_1^2-1)^{\gamma-1}\cos\theta_1]/[(u_1^2-1)^{\gamma}\cos\theta_1 - w_a] - 1\right\}}{\left\{\cos^2\theta_1 + [u_1^2(u_1^2-1)^{\gamma-1}\cos\theta_1]/[(u_1^2-1)^{\gamma}\cos\theta_1 - w_a]u_1^8\sin^2\theta_t\right\}}, \quad (9.14)$$

$$w_{au} = \frac{(u_1^2-1)^{\gamma}}{\cos\theta_1}, \quad (9.15)$$

and

$$w_{al} = -\frac{(u_1^2-1)^{\gamma}}{u_1^3\cos\theta_{ul} - 1}, \quad (9.16a)$$

where

$$\cos\theta_{ul} = \left[1 - \sin^2\theta_t\right]^{1/2}. \quad (9.16b)$$

In the above relations θ_n denotes the angle of the imposed bed slope S and θ_{ul} denotes the bed angle at $x = 0$ (and $u = 1$) in the limit as $w \to w_{al}$. Finally, the relation (3.28b) for conjugate velocity just upstream of the hydraulic jump is replaced with the imposition of the condition

$$M(u) = 0 \quad \text{at} \quad x = L, \quad (9.17a)$$

where

$$M(u) = u^{-3}\cos\theta - u^{-1}(\cos\theta_u + 2Fr_t^2) + 2Fr_t^2 = 0, \quad (9.17b)$$

and θ_u denotes the bed angle at $x = 0$, given by

$$\tan\theta_u = -\frac{w_a}{c}\sin\theta_t. \quad (9.17c)$$

It can easily be shown that all of the above finite-slope generalizations reduce to the corresponding previously introduced infinitesimal-slope forms in the limit of small angle. In the case of the infinitesimal-slope theory, however, the friction coefficient C_f could be absorbed into the streamwise coordinate in accordance with (3.21d) and (3.7a), allowing for a universal formulation independent of C_f. This is no longer possible in the case of the finite-slope formulation, as can be seen, for example, from (9.10b).

The numerical solution can be implemented in the same way as that for the case of negligible slope. In order to facilitate this it is useful to solve (9.8) for bed slope:

$$\tan\theta = \sin\theta_t \frac{(u^2-1)^{\gamma}\left\{1 + \sin^2\theta_t[w_a^2 - (u^2-1)^{2\gamma}]/c^2\right\}^{1/2} - w_a}{c\left[1 - \sin^2\theta_t(u^2-1)^{2\gamma}/c^2\right]}. \quad (9.18)$$

It can be seen that (9.18) is the generalization of (3.23).

The most important result of the finite-slope analysis is not the forms of the steps themselves, which prove to be relatively insensitive to geometric nonlinearities. It is rather in the delineation of a friction coefficient C_f beyond which the present analysis breaks down. In particular the bed attains infinite slope wherever flow velocity becomes so high that the denominator of (9.18) vanishes. (The equation also becomes invalid when the argument inside the surd becomes negative, but this requires a higher velocity than the one which causes the denominator to vanish). If the denominator of (9.18) vanishes at a velocity u that is lower than the one which causes the function M of (9.17b) to vanish, bed slope becomes infinite upstream of the point where the velocity would be high enough to enable the hydraulic jump that allows a cyclic solution.

The critical condition for the existence of cyclic solutions is thus one for which the value of u causing the denominator to vanish (and thus $\tan\theta$ to become infinite) is

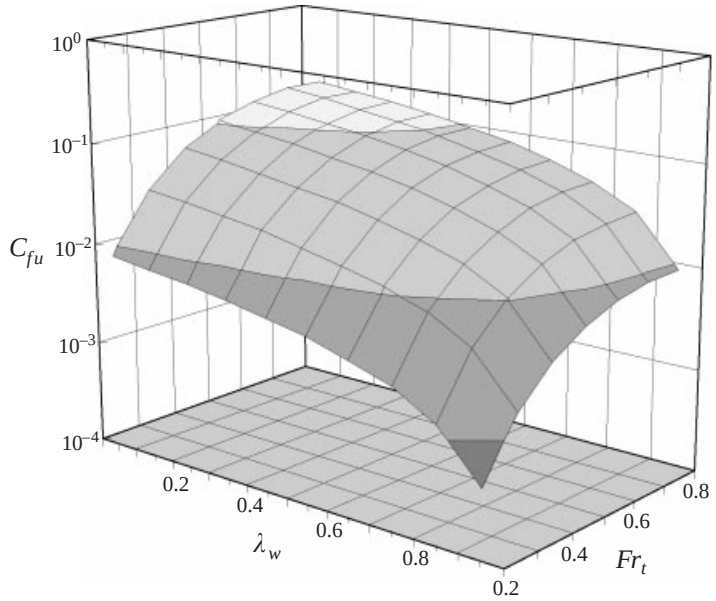

FIGURE 16. Plot of the upper bound C_{fu} on the friction coefficient for the existence of solutions for cyclic steps as a function of Fr_t and $\lambda_w = (w_a - w_{al})/(w_{au} - w_{al})$, for the case $\gamma = 1.5$.

equal to the value of u that causes M to vanish. From (9.18), (9.7) and (9.11) this can be reduced to the following upper bound C_{fu} on the friction coefficient C_f:

$$C_{fu} = \frac{(u_1^2 - 1)^\gamma - w_a \cos\theta_1}{\cos\theta_1 (u_c^2 - 1)^\gamma}, \tag{9.19}$$

where u_c is the conjugate velocity obtained from (9.17b) at an angle θ of 90°:

$$u_c = \frac{2Fr_t^2 + \cos\theta_u}{2Fr_t^2}. \tag{9.20}$$

For any specified values of Fr_t and w_a the limit C_{fu} can be easily found by simple successive approximation from (9.19) with the aid of (9.20), (9.7), (9.10), (9.11) and (9.17c).

The limit C_{fu} was computed over the range defined by $Fr_t \in [0.2, 0.8]$ and $w_a \in (w_{al}, w_{au})$ for the case $\gamma = 1.5$. It is worth mentioning that the values of w_{al} and w_{au} predicted by the finite-slope relations varied no more than 4% from the corresponding values from the theory for infinitesimal slope. Figure 16 shows C_{fu} as a function of Fr_t and λ_w, where

$$\lambda_w = \frac{w_a - w_{al}}{w_{au} - w_{al}}, \tag{9.21}$$

and the values of w_{au} and w_{al} are those of the theory for infinitesimal slope. Note that λ_w is defined so that it equals zero when $w_a = w_{al}$ and unity when $w_a = w_{au}$.

For a large threshold Froude number Fr_t of 0.8 and a small value of λ_w of 0.05 it is found that C_{fu} is as large as 0.167, indicating an extremely broad range over which cyclic steps can form. At opposing limit of $Fr_t = 0.2$ and $\lambda_w = 0.95$, C_{fu} is as small as 0.00044, indicating that solutions for cyclic steps can be obtained only for unrealistically smooth surfaces.

Fr_t	w_a	C_{fu}	C_f	$(Fr_n)_f/(Fr_n)_i$	$(c)_f/(c)_i$	$(\Delta\eta)_f/(\Delta\eta)_i$	$(L)_f/(L)_i$
0.2	−0.6	0.00875	0.001	1.0012	1.0000	1.0025	1.0000
0.2	−0.6	0.00875	0.0085	1.0237	1.0000	1.0456	0.9976
0.4	0	0.0577	0.005	1.0005	1.0000	1.0011	1.0000
0.4	0	0.0577	0.04	1.0207	0.9997	1.0401	0.9968
0.6	0.5	0.0455	0.005	1.0006	1.0000	1.0011	0.9998
0.6	0.5	0.0455	0.04	1.0970	0.9983	1.2227	1.0136

TABLE 4. Ratio of value predicted by the finite-slope formulation to that predicted by the infinitesimal-slope formulation for several of the parameters of the cases of table 2. Also listed is the resistance coefficient used in the calculation and the upper limit for resistance coefficient. The exponent γ is equal to 1.5.

Fr_t	w_a	C_{fu}	C_f	$(\theta_{max})_i$ (deg.)	$(\theta_{max})_f$ (deg.)
0.2	−0.6	0.00875	0.001	6.4	6.5
0.2	−0.6	0.00875	0.0085	35.4	71.8
0.4	0	0.05772	0.005	4.2	4.2
0.4	0	0.05772	0.04	30.5	37.8
0.6	0.5	0.04548	0.005	3.3	3.3
0.6	0.5	0.04548	0.04	24.9	32.2

TABLE 5. Maximum angle of inclination predicted by the finite-slope and infinitesimal slope formulations for the cases of table 4. The exponent γ is equal to 1.5.

Several of the cases explored with the infinitesimal-slope theory and presented in tables 3 are revisited in tables 4 and 5 using the finite-slope theory. In table 4 the four dimensionless parameters Fr_n, c, L and $\Delta\eta$ are revisited for the case $\gamma = 1.5$. For each specified pair (Fr_t, w_a) the ratio of the value of each of these four parameters predicted by the finite-amplitude theory for a specified value of C_f to the value predicted by the infinitesimal-amplitude theory is compared. Two cases are considered for each pair (Fr_t, w_a), one for which C_f is well below C_{fu} and another for which C_f is near C_{fu}. It is seen from the table that the predictions of the infinitesimal-slope theory are surprisingly accurate until C_f becomes very close to C_{fu}.

This conclusion is confirmed in table 5, in which the predictions for the maximum bed angle θ_{max}, attained just before the hydraulic jump, for the finite-slope formulation are compared with the corresponding predictions for the infinitesimal-slope formulation. The agreement is all the more remarkable in that θ_{max} is likely to be the parameter most poorly described by the infinitesimal-slope theory. The infinitesimal-slope theory performs poorly in terms of θ_{max} only in the case $(Fr_t, w_a, C_f) = (0.2, -0.6, 0.0085)$; the value of C_f in this case is very close to the upper limit C_{fu} of 0.00875.

A comparison of the bed profiles predicted by the finite-slope and infinitesimal-slope theories is presented in figure 17 for the case $(\gamma, Fr_t, w_a, C_f) = (1.5, 0.6, 0.5, 0.04)$ of tables 4 and 5. The value for C_{fu} in this case is 0.0455. The plot is given in terms of

$$\hat{x}_s = \frac{x_s}{\sin\theta_t} \tag{9.22}$$

rather than $\hat{x} = x/\sin\theta_t$ so as to ensure that the Froude-critical point is reached at the same point, i.e. $\hat{x}_s = 0$ in both plots. Again the agreement is seen to be very close except in a short zone of very steep bed just before the hydraulic jump.

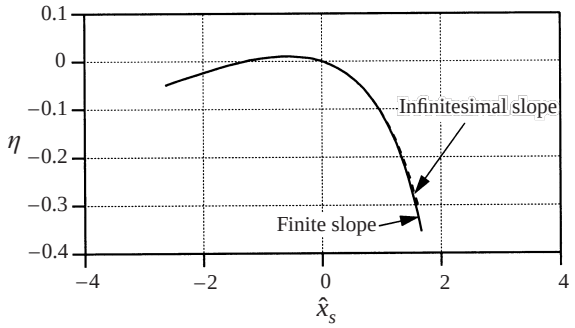

FIGURE 17. Plot of the dimensionless bed profile predicted by the infinitesimal-slope theory of the case $(Fr_t, w_a) = (0.6, 0.5)$ with that predicted by the finite-slope theory for the case $(Fr_t, w_a, C_f) = (0.6, 0.5, 0.04)$, for $\gamma = 1.5$. The associated upper bound C_{fu} in this case is 0.0455. The Froude-critical point occurs at $\hat{x}_s = 0$.

Several of the equations presented previously for the infinitesimal-slope case must be modified for the finite-slope case. Rather than reintroduce them, the required changes are indicated here. In (3.5*a*), (3.5*b*) and (3.9) the right-hand side must be divided by $\cos\theta_n$. In (3.8) and (3.9) S_r must be replaced by $\sin\theta_n/\sin\theta_t$. In (3.10), (3.11), (5.10) and (5.14) S_t must be replaced with $\sin\theta_t$. In (5.12) c must be replaced with $c/\cos\theta_n$. The generalizations to (5.13*a*) and (5.13*b*) are

$$\xi_d = \eta_d + \frac{h_d}{\cos\theta} = \eta_d + \frac{q_w}{u_d\cos\theta}, \tag{9.23a}$$

$$\xi = \frac{u_t}{q_w}\xi_d = \eta + (u\cos\theta)^{-1}. \tag{9.23b}$$

10. Comparison with data and sample calculation

Although a variety of experimental and field research on headcut formation in cohesive material has been performed, including the work of Holland & Pickup (1976), Gardner (1983) and Stein & Julien (1993), none lends itself to a direct test of the validity of the above theory. This is due to the lack of an empirically determined form of the erosion relation (3.1) for the material in question. In addition, the research of Gardner (1983) and Stein & Julien (1993) pertains to single steps. That of Holland & Pickup (1993) pertains to multiple steps, but their location is determined by an imposed vertical variation in erodibility. The only experimental work that demonstrates the existence of purely erosional cyclic steps is due to Sawai (1977) and Koyama & Ikeda (1998). Here again, though, the data are not sufficient to allow a general determination of a form for the erosion relation.

This notwithstanding, several reasonable assumptions can be made so as to apply the present theory to the experiments of Sawai (1977). An erosional relation of the form of (3.1) is assumed, in which γ is taken to be 2. In addition, the value of u_t in (3.2) is taken to be $7\,\mathrm{cm\,s^{-1}}$. Sawai reports that in one of the experiments, before steps formed a flow depth of 4.5 mm was realized for a water discharge per unit width of $30\,\mathrm{cm^2\,s^{-1}}$ on a slope of 26°. The friction coefficient C_f for this case can thus be estimated as 0.043. Though the friction coefficient can be expected to be a weak function of flow depth and roughness height and therefore should differ for each run, the above-quoted value is used for all runs for lack of better information. In table 6 observed values of dimensional step length L_d are compared against computed ones.

Run	$\sin\theta_n$	Discharge per unit width, q_w ($cm^2\ s^{-1}$)	Fr_t	Fr_n	Observed wavelength, L_d(cm)	Predicted wavelength, L_d(cm)	w_a
1	0.225	3.85	0.302	2.29	8.9	2.93	10.7
2	0.225	7.50	0.216	2.29	6.3	13.4	23.1
3	0.225	9.09	0.196	2.29	5.5	20.3	28.0
4	0.438	2.22	0.397	3.19	3.6	0.335	5.31
5	0.438	3.85	0.302	3.19	4.4	1.35	13.0
6	0.438	5.88	0.244	3.19	4.7	3.61	23.5
8	0.707	2.50	0.374	4.05	4.2	0.273	6.84
9	0.707	4.17	0.290	4.05	2.6	0.965	15.8
10	0.545	7.69	0.213	3.56	6.3	5.15	35.5
11	0.555	13.3	0.162	3.59	15	16.4	68.7
12	0.196	6.67	0.229	2.13	14	12.2	18.6

TABLE 6. Results of an application of the present theory to the experiments of Sawai (1977).

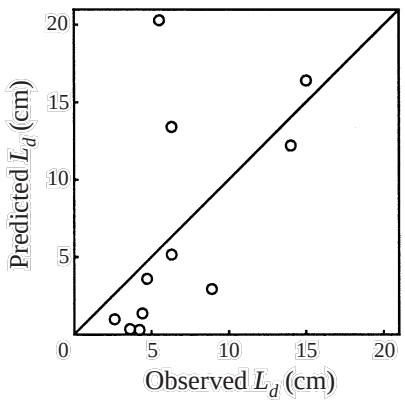

FIGURE 18. Values of L_d predicted by the theory plotted against the values observed in the experiments of Sawai (1977).

All cases of table 1 are included in the calculation except for Run 7, for which L_d was not measured. In the calculations, in lieu of better information the discharge per unit width was approximated as the discharge divided by the water surface width. A comparison between observed and predicted step wavelength is shown in figure 18. Because the predicted wavelength is a sensitive function of u_t, which is in turn strongly influenced by several vagaries associated with cohesive soil including water content, time of drying, ionic content of pure water etc., the comparison must be considered approximate at best. This notwithstanding, the agreement between observed and predicted values of step length L_d is acceptable in the light of the above-noted limitations.

In order to illustrate the application of the theory a sample calculation is presented here for the case $(\gamma, Fr_t, w_a, C_f) = (1.5, 0.6, -0.3, 0.04)$. The value of C_{fu} in this case is 0.123, a value that is in the present case sufficiently large compared to C_f to render the predictions of the infinitesimal-slope theory highly accurate. This notwithstanding, all calculations were performed using the finite-slope theory. The predicted values of the dimensionless normal Froude number Fr_n, wave speed c, wavelength L, wave height

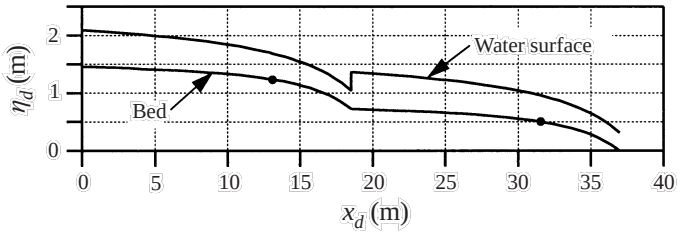

FIGURE 19. Dimensional plot of cyclic steps for the case $(\gamma, Fr_t, w_a, C_f) = (1.5, 0.6, -0.3, 0.04)$ and $u_t = 1.5\,\mathrm{m\,s^{-1}}$. The dots denote the Froude-critical points.

$\Delta\eta$, step sharpness s, angle of average bed slope between the Froude-critical point and the hydraulic jump θ_f and maximum bed angle θ_{max} were found to be 0.994, 0.455, 0.418, 1.15, 6.43, 5.3° and 11.4°, respectively. The critical bed slope $S_t = \tan\theta_t$ and normal bed slope $S = \tan\theta_n$ are found to be 0.0144 and 0.0395, respectively.

In order to explore the implications of the theory at field scale, it is assumed that the threshold velocity for bed erosion u_t is $1.5\,\mathrm{m\,s^{-1}}$. With the aid of (2.2) and (3.7*b*) this yields a value of $0.956\,\mathrm{m^2\,s^{-1}}$ for q_w and a value of 0.637 m for h_t. Dimensional step length L_d is thus found from (9.6*a*) to be 18.5 m. Dimensional step height $\Delta\eta_d$ is found from (3.21*b*) to be 0.731 m. Two wavelengths of bed and water surface elevation profiles are plotted in dimensional form in figure 19.

Further calculations require a value for the coefficient α in the erosion relation (3.3). Here this is done by imposing a vertical erosion rate w_{nd} in the absence of steps of $1\,\mathrm{mm\,h^{-1}}$. It is seen from (3.6) that this corresponds to a wave speed c_{nd} of $25.3\,\mathrm{mm\,h^{-1}}$. Assuming the porosity λ_p to be equal to 0.3, α can be back-calculated from the finite-slope generalization of (3.5*a*) to yield a value of $0.0745\,\mathrm{mm\,h^{-1}}$. The predicted values of c_{sd} and w_{sd} are thus found from (5.11), the finite-slope generalization of (5.12) and (9.6*b*) to be $33.6\,\mathrm{mm\,h^{-1}}$ and $1.01\,\mathrm{mm\,h^{-1}}$, respectively. Note that in this case the wave speed is noticeably elevated, and the degradation rate slightly elevated in the presence of steps.

11. Conclusion

A complete theory is presented for purely erosive one-dimensional cyclic, or periodic steps in cohesive material of uniform erodibility. These features are trains of headcuts which degrade and migrate upstream at constant rates, preserving their form as they do so. Each step is characterized by an upstream region of subcritical flow and a downstream region of supercritical flow ending in a hydraulic jump. As step sharpness increases, the relative length of the zone of subcritical flow increases at the expense of that of supercritical flow.

Once the friction coefficient and the parameters of the erosion relation are specified, the theory allows the prediction of all relevant parameters, including wavelength, wave height, wave speed, degradation rate, and bed and water surface profiles. In addition to the exponent γ of the erosion relation, the two most important dimensionless parameters governing the phenomenon are the Froude numbers Fr_t and Fr_n associated with flow velocity at the threshold of motion and normal flow velocity in the absence of steps, respectively. Step sharpness increases as Fr_t decreases and Fr_n increases.

Erosional steps are related to the erosional version of the antidune mechanism. A linear stability analysis of this mechanism suggests that a necessary condition for the spontaneous formation of steps is that $Fr_t > 1$, i.e. that the normal flow in the

absence of steps be supercritical. Steps can still exist for subcritical values of Fr_n as long as $Fr_t < Fr_n$. In this range, however, a finite-amplitude perturbation is necessary to trigger them. The case of a solitary step is obtained in the limit as $Fr_n \to Fr_t$. This form, which has infinite wavelength, is also self-preserving as it migrates upstream.

A consideration of geometric nonlinearities leads to the specification of an upper limit to the resistance coefficient beyond which the theory breaks down. The theory fails at this limit because the bed slope becomes infinite just upstream of the hydraulic jump. An infinitesimal-slope theory that neglects geometric nonlinearities, however, performs quite well up to values of the resistance coefficient that are not far below the limit value. The fact that the present theory breaks down for sufficiently large resistance coefficient may not mean that cyclic steps cannot form under such conditions. It may instead mean that a bed shock in the form of a waterfall needs to be included in the analysis. This observation suggests a further research topic.

The research presented here on purely erosional cyclic steps, combined with the recognition of an analogous transportational form in fine non-cohesive material (e.g. Winterwerp *et al.*1992) suggests an underlying similarity between the two phenomena. The pursuit of a unified theory of cyclic steps promises to be an exciting research topic for the future.

The first author deeply thanks Steve Crouch and John Gulliver for granting the two leaves of absence that made his contribution to this research possible. Syunsuke Ikeda kindly made facilities available to him at the Tokyo Institute of Technology on the occasion of the second leave of absence. Numerous discussions with Bill Dietrich, Leslie Reid and Kazuo Taki are gratefully acknowledged. Juichiro Akiyama kindly supplied some of the Japanese papers. Support from the National Science Foundation (CTS-9207882) is likewise greatly appreciated.

REFERENCES

Ariathurai, R. & Arulanandan, K. 1978 Erosion rates of cohesive soil. *J. Hydraul. Engng ASCE* **104**(HY2), 279–283.

Ashida, K., Egashira, S. & Nishimoto, N. 1986 Sediment transport mechanism on step-pool bed form. *Annuals, Disaster Prevention Research Institute, Kyoto University, Japan* **29**(B-2), 1–14 (in Japanese).

Ashida, K. & Sawai, K. 1977 A study on the stream formation process on a bare slope. (3) Three-dimensional channel form. *Annuals, Disaster Prevention Research Institute, Kyote University, Japan* **20**(B-2), 1–15 (in Japanese).

Blong, R. J. 1970 The development of discontinuous gullies in a pumice catchment. *J. Sci.* **268**, 369–383.

Colombini, M., Seminara, G. & Tubino, M. 1987 Finite-amplitude alternate bars. *J. Fluid Mech.* **181**, 213–232.

Croad, R. N. 1981 Physics of erosion of cohesive soils. *Rep.* 247. Dept. of Civil Engineering, University of Auckland, New Zealand.

Engelund, F. 1970 Instability of erodible beds. *J. Fluid Mech.* **42**, 225–244.

Foster, G. R. & Meyer, L. D. 1975 Mathematical simulation of upland erosion using fundamental erosion mechanics. *Proc. 1972 Sediment Yield Workshop*, pp. 190–207. US Dept. of Agriculture, Agricultural Research Service, ARS-S40.

Fredsoe, J. 1974 On the development of dunes in erodible beds. *J. Fluid Mech.* **64**, 1–16.

Gardner, T. W. 1983 Experimental study of knickpoint and longitudinal profile evolution in cohesive, homogeneous material. *Geol. Soc. Am. Bull.* **94**, 664–672.

Grant, G. E. & Mizuyama, T. 1991 Origin of step-pool sequences in high-gradient streams: a flume experiment. *Proc. Japan-US Workshop on Snow Avalanche, Landslide, Debris Flow*

(ed. Y. Hagiwara), pp. 523–532. National Research Institute for Earth Science and Disaster Prevention, Science and Technology Agency, Tsukuba, Japan.

Holland, W. N. & Pickup, G. 1976 Flume study of knickpoint development in stratified sediment. *Geol. Soc. Am. Bull.* **87**, 76–82.

Howard, A. D. 1994 A detachment-limited model of drainage-basin evolution. *Wat. Resour. Res.* **30**, 2261–2285.

Izumi, N. & Parker, G. 2000 Linear stability analysis of channel inception: downstream driven theory. *J. Fluid Mech.* **419**, 239–262.

Johanesen, C., Larsen, T. & Petersen, O. 1994 Experiments on the erosion of mud from the Danish Wadden Sea. In *Cohesive Sediments* (ed. N. Burt, W. R. Parker and J. Watts). *Proc. 4th Nearshore and Estuarine Cohesive Sediment Transport Conference, INTERCOH '94, Wallingford, UK*, Paper 24, 10pp. John Wiley, Chichester.

Kennedy, J. F. 1963 The mechanics of dunes and antidunes in erodible bed channels. *J. Fluid Mech.* **16**, 521–544.

Koyama, T. & Ikeda, H. 1998 Effect of riverbed gradient on bedrock channel configuration: a flume experiment. *Proc. Environmental Research Center, Tsukuba University, Japan* **23**, 25–34.

Leopold, L. B. & Miller, J. P. 1956 Ephemeral streams-hydraulic factors and their relation to the drainage net. *US Geological Survey Professional Paper* 282-A, 36pp.

Montgomery, D. R. & Dietrich, W. B. 1989 Source areas, drainage density and channel initiation. *Wat. Resour. Res.* **25**, 1907–1918.

Otsubo, K. & Muraoka, K. 1982 Study on the pickup rate of cohesive material. *Proc. 26th Annual Hydraulics Conference, Japan Society of Civil Engineering*, pp.141–146 (in Japanese).

Reid, L. M. 1989 Channel incision by surface runoff in grassland catchments. PhD Thesis, University of Washington.

Sawai, K. 1977 Sediment hydraulics research on the mechanism of variation of the bed of cohesive channels. PhD thesis, Kyoto University (in Japanese).

Schielen, R., Doelman, A. & Swaart, H. E. De 1993 On the nonlinear dynamics of free bars in straight channels. *J. Fluid Mech.* **252**, 325–356.

Sheng, Y. P. & Lick, W. 1978 The transport and resuspension of sediments in a shallow lake. *J. Geophys. Res.* **84**, 1809–1826.

Simons, D. B., Richardsonk, E. V. & Nordin, C. F. 1965 Sedimentary structures generated by flow in alluvial channels. *Soc. Econ. Paleo. Mineralogists, Special Pub.* 12, 21pp.

Stein, O. R. & Julien, P. Y. 1993 Criterion delineating the mode of headcut migration. *J. Hydraul. Engng ASCE* **119**, 37–49.

Teisson, C., Ockenden, M., Le Hir, P., Kranenburg, C. & Hamm, L. 1993 Cohesive sediment transport processes. *Coastal Engng* **21**, 129–162.

Umita, T., Kusuda, T., Futawatari, T. & Awaya, Y. 1988 Study on erosional processes of soft mud. *Proc. Japan Society of Civil Engineering* **393**, 33–42 (in Japanese).

Whittaker, J. G. & Jaeggi, M. N. R. 1982 Origin of step-pool systems in mountain streams. *J. Hydraul. Engng* **108**, 758–773.

Winterwerp, J. C., Bakker, W. T., Mastbergen, D. R. & Van Rossum, H. 1992 Hyperconcentrated sand-water mixture flows over erodible bed. *J. Hydraul. Engng ASCE* **119**, 1508–1525.